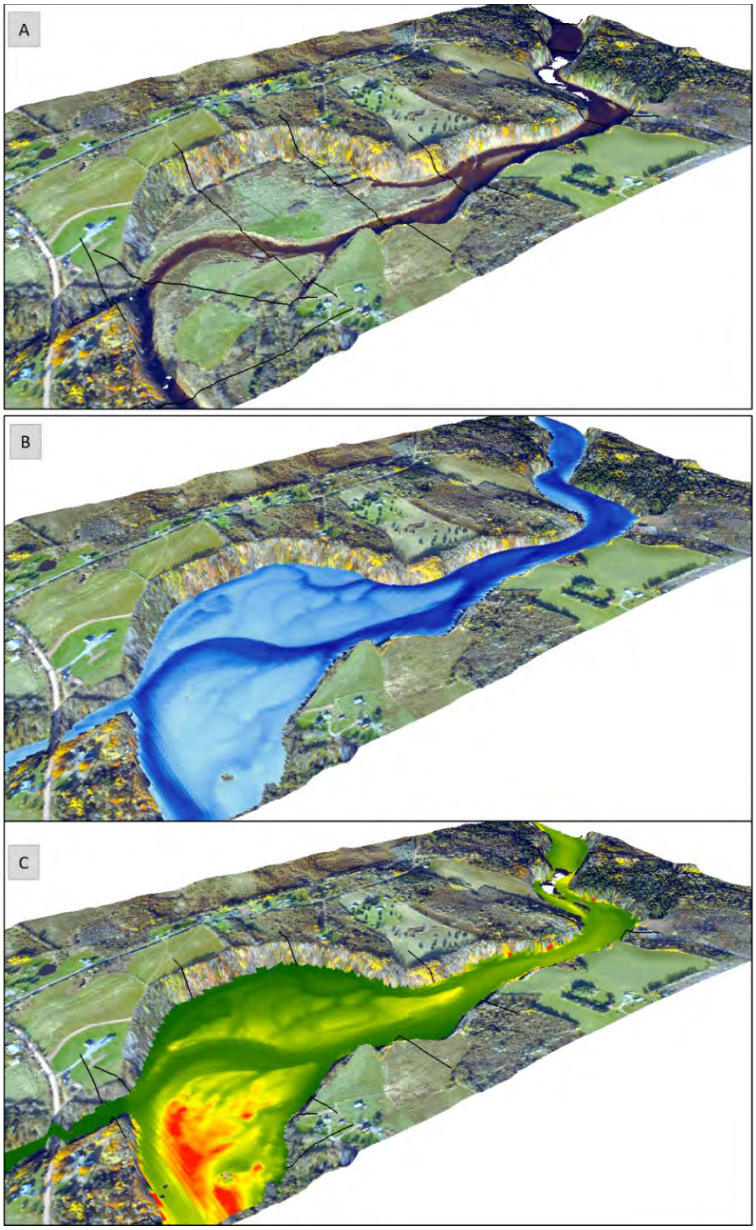

Topo-bathymetric survey for Hydrodynamic Modeling - River John

Prepared by
Timothy Webster, PhD,
Nathan Crowell,
Dedipya Kodavati, et al.
Applied Geomatics Research Group
NSCC, Middleton
Tel. 902 825 5475
email: tim.webster@nscc.ca

Submitted to:

GeoNOVA & NS Department of Municipal Affairs

How to cite this work and report:

Webster, T., Crowell, N. and Kodavati, D. 2020. “Topo-bathymetric survey for Hydrodynamic Modeling - River John” Technical Report submitted to GeoNova and NS Department of Municipal Affairs, Applied Geomatics Research Group, NSCC Middleton, NS.

Table of Contents

List of Figures

List of Tables

Executive summary

The Applied Geomatics Research Group (AGRG) part of Nova Scotia Community Colleges Applied Research has expertise in conducting Topo-bathymetric lidar surveys in Atlantic Canada. In partnership with GeoNOVA and the NS Department of Municipal Affairs, AGRG was chosen to prepare a document describing the role and value of topo-bathymetric lidar (TB-lidar) for inland and coastal flood risk mapping in Nova Scotia. As a part of this study a TB-lidar river survey was conducted on October 29th, 2019 for River John in Pictou County, NS. Part of the aerial survey campaign involves flying over the active GNSS control base station prior to and directly following the survey. In this case the Tatamagouche active control station was used as it had been in previous surveys in the area. Unfortunately, it was later determined during post-processing of the aircraft trajectory that it was determined that the Tatamagouche station had been moved and was not operational during the flight. As a result of this active control stations farther from the survey site were used, New Glasgow and Pugwash, which increased the baseline of the trajectory to the upper limits and resulted in a degraded positional accuracy of the aircraft trajectory. The main objective of this study was to prepare a hydrodynamic model for fluvial flooding using MIKE 11 and MIKE 21 models. In-situ data such as ground truthing information, Secchi depths and water samples were collected during the summer. Survey grade GNSS validation check points were collected on hard surfaces for the topographic lidar and river cross-sections for the bathymetric lidar. These check points were used to validation the elevations of the two lidar sensors utilized in the TB-lidar survey. Results indicate the topographic and bathymetric lidar met the vertical specifications with accuracies getter than 15 cm. Two pressure sensors were installed in the river's intertidal zone and their data were used to validate the simulation results for Hurricane Dorian which passed through the study site on September 7th and 8th, 2019. In order to minimize the run time, the model ran for a span of four days Sep 5th to 9th, 2019 capturing the storm surge and rainfall event. Also included were the 1:100 year and three times a 1:100-year magnitude rain event in the MIKE 11 model. Flood hazard maps were produced after linking one-dimensional hydrodynamic model to the two-dimensional hydrodynamic model.

1 Introduction

1.1 Project background

The main purpose of this project was to develop Topo-bathymetric lidar guidelines for flood risk mapping in Nova Scotia, which involved conducting a Topo-bathymetric lidar river survey of the River John in Pictou County for hydrodynamic modelling. This project was granted to AGRG by GeoNOVA in 2019 with funding from the NS Department of Municipal Affairs. This document outlines the data collected and discusses in detail the hydrodynamic modelling executed using the MIKE suite of software from the Danish Hydraulic Institute (DHI) for the study site.

1.2 Study area

The study area of River John in Pictou County, Nova Scotia (Figure 1.1) was selected to demonstrate the value of topo-bathymetric lidar for fluvial flood risk mapping. The river is located on the North Shore of mainland Nova Scotia and empties into the Northumberland Strait, the water has relatively low turbidity and offers good conditions for topo-bathymetric lidar surveys.

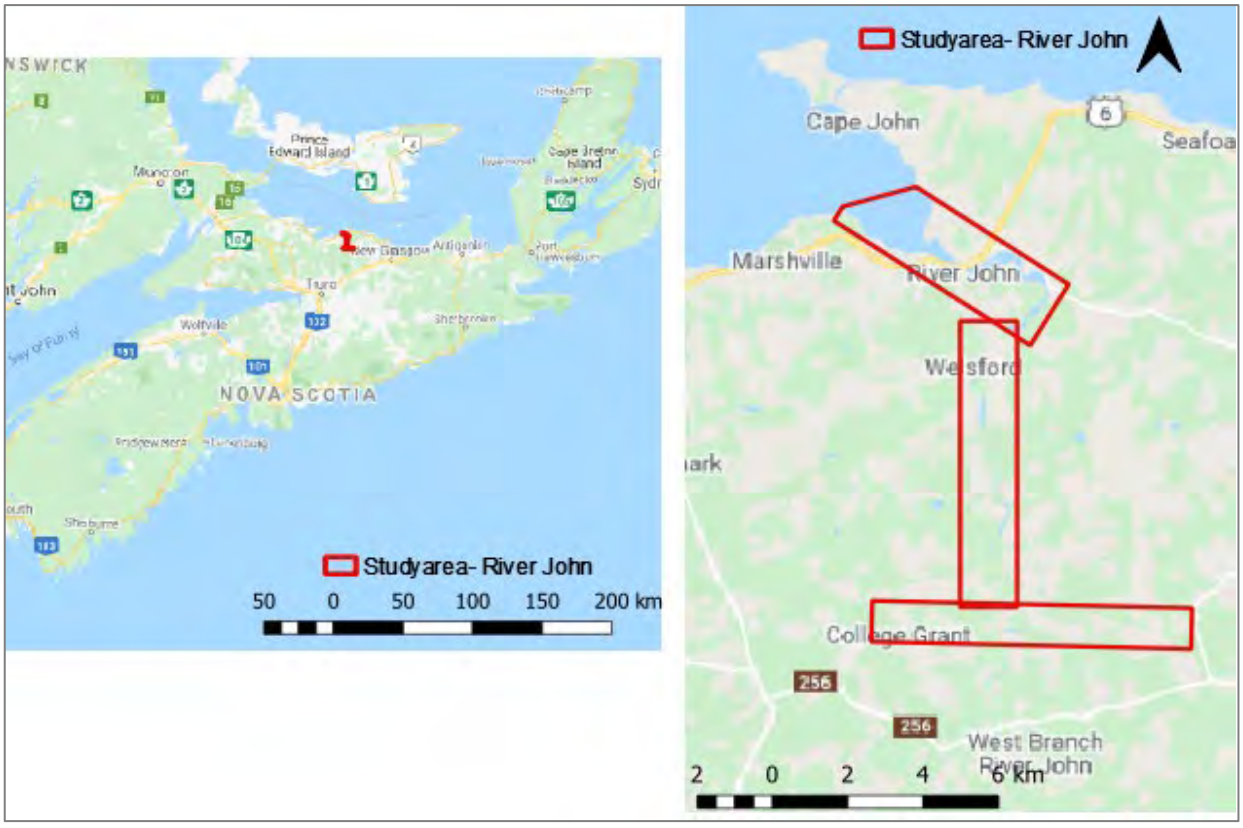

Figure 1.1 Topo-bathymetric lidar study area- River John (background Google maps).

2 Methods

2.1 Sensor Specifications

The lidar sensor used in this study was a Chiroptera II integrated topographic-bathymetric sensor equipped with a 60-megapixel multispectral camera. The system incorporates a 1064 nm near-infrared laser for ground returns and water surfaces, and a green 515 nm laser for bathymetric returns (Figure 2.1, Figure 2.2d). The lasers scan in an elliptical pattern, which enables coverage from many different angles on vertical faces, causes less shadow effects in the data, and is less sensitive to wave interaction. The bathymetric laser is limited by water depth and clarity and has a penetration rating of roughly 1.5 x the Secchi depth (a measure of turbidity or water clarity using a black and white disk). The Leica RCD30 60 megapixel camera (Figure 2.2d) collects co-aligned RGB+NIR motion compensated photographs which can be mosaicked into a single image in post-processing, or analyzed frame by frame for maximum information extraction.

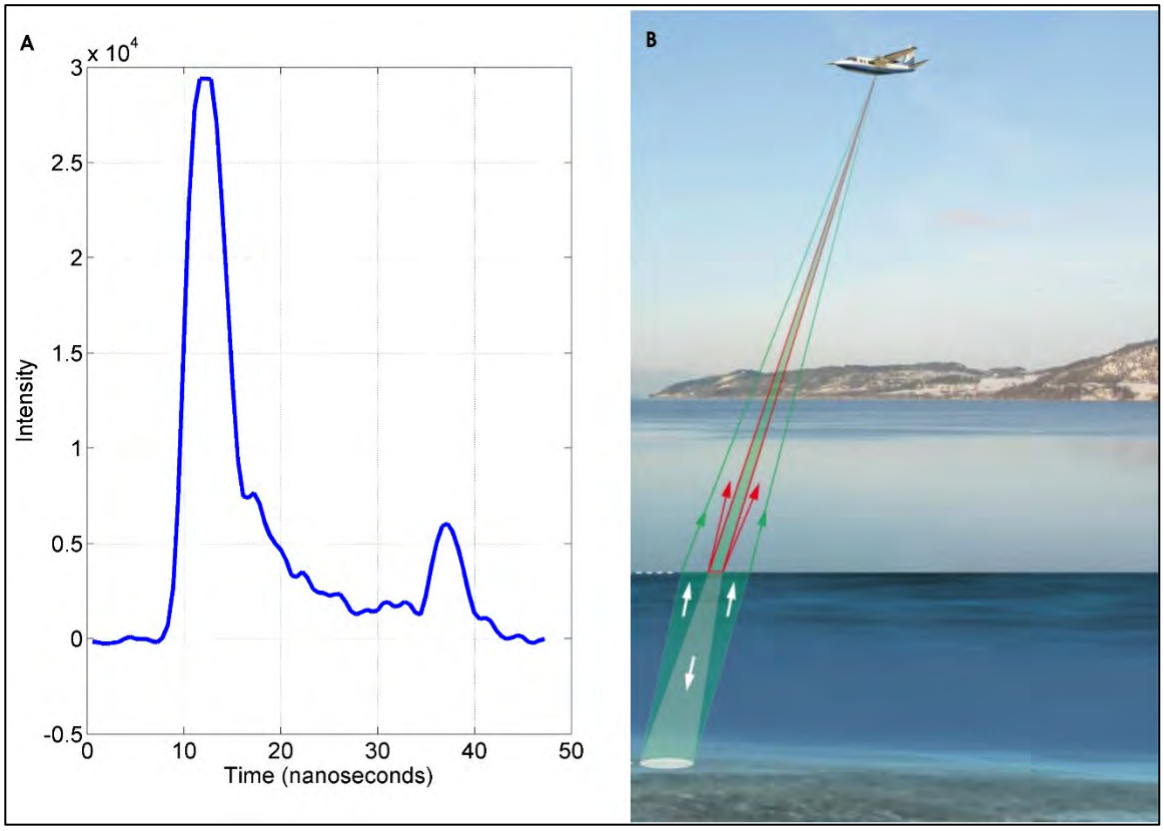

Figure 2.1: (A) Example of the Chiroptera II green laser waveform showing the large return from the sea surface and smaller return from the seabed. (B) Schematic of the Chiroptera II green and NIR lasers interaction with the sea surface and seabed (adapted from Leica Geosystems).

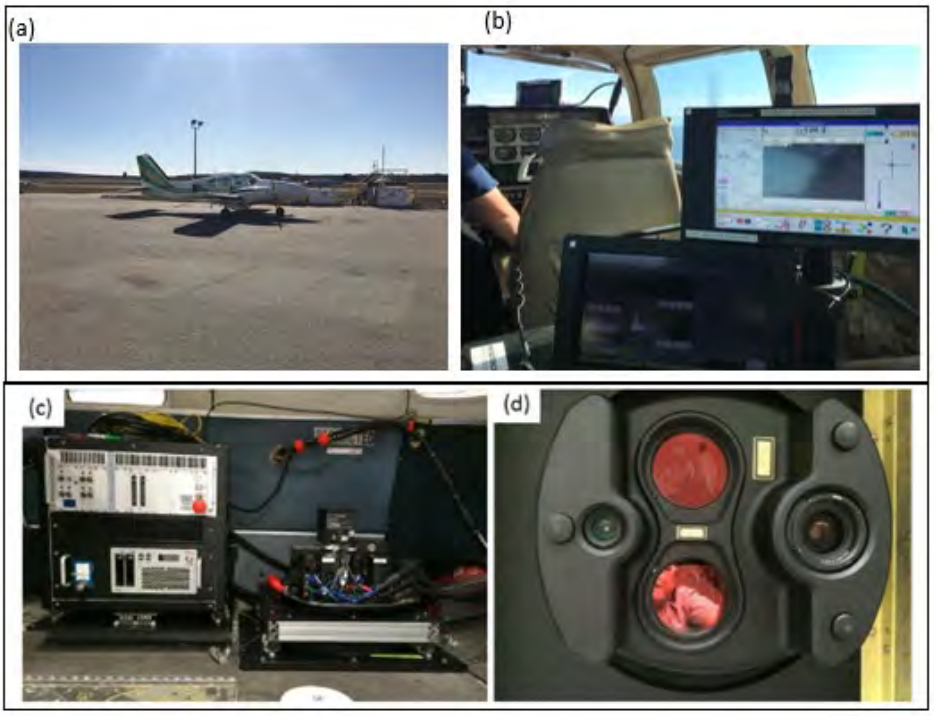

Figure 2.2: (a) Aircraft used for 2019 lidar survey; (b) display seen by lidar operator in-flight; (c) main body of sensor (right) and the data rack (left); (d) large red circles are the lasers; the RCD30 lens (right) and low resolution camera quality control (left).

2.2 Lidar Survey Details

AGRG rented an America Piper Aztec (AGRG-NSCC does not own an aircraft, only the sensor) from Air America through a collaboration with Leading Edge Geomatics. The aircraft arrival time was set back several times and the delays resulted in the operation beginning in mid-October when initially they were expected to start in late-July-early August. The lidar sensor was installed in the twin engine aircraft in Fredericton, NB. Since the study area is small only a day was needed to conduct the lidar survey using the Chiroptera II sensor with both the topo and bathy scanners. The survey took place on October 29th, 2019 and was planned using Mission Pro software. It was flown at an altitude of 400 m and took a total of 3 hours to collect 26 flight lines. The lidar sensor requires ground-based high precision Global Positioning System (GPS or GNSS) data to be collected during the lidar survey in order to provide accurate positional data for the aircraft trajectory. The Nova Scotia Active Control Stations (NSACS) cellular network was used to provide geodetic control during the survey and was used to process the trajectory of the survey aircraft (Figure 2.3). The NSACS network was also used to establish base station coordinates for real-time kinematic collection of ground truth data within the study area. Part of the flight operation includes flying “flat and level” over the base station and then as one approaches the survey site to conduct a figure 8 flight pattern to ensure the inertial measurement unit is “warmed up” and working correctly prior to beginning the survey. Previous surveys in this area have utilized the Tatamagouche

active control station, which is the closest to the survey site, and was used again during this survey as can be seen in the survey flight trajectory. Initially the active control station in Tatamagouche TATA (250029) was chosen to process the trajectory using Inertial Explorer software but after trying to download data for the time period of the survey, it was discovered that this station was moved to a new location and the new coordinates were not published, hence the trajectory has to be processed using Pugwash and New Glasgow stations which are approximately 30 km away from the survey site. The operational procedure of flying over the base station was not accomplished because of the lack of information concerning the no-operational TATA (250029) NSACS.

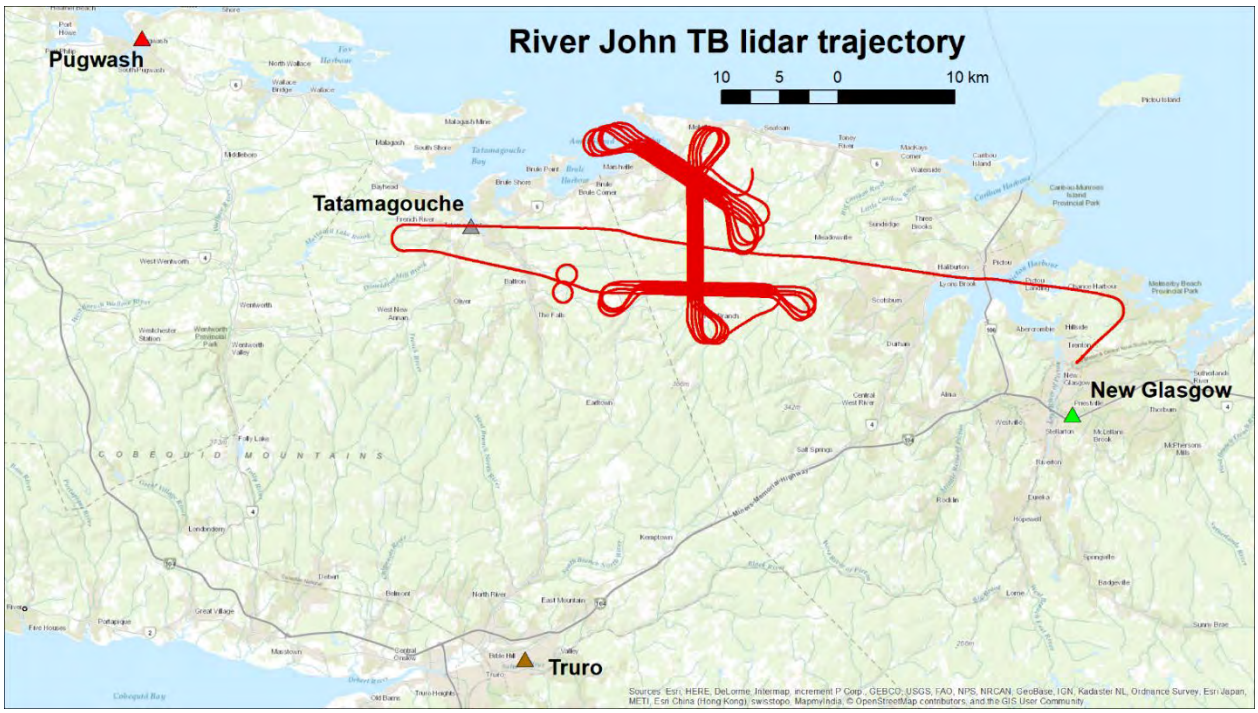

Figure 2.3: Aircraft actual surveyed flight lines for the lidar survey in River John in red, and also showing NSACS stations nearby. The survey was executed under the assumption that the Tatamagouche active control station was operational at the time.

The topographic (topo) lidar was set to pulse at 500 kHz and the bathymetric (bathy) lidar was set to pulse at 35 kHz. A recent upgrade to the processing software allowed the bathymetric lidar to collect and process four times the number of points that are usually collected, thus effectively providing a pulse repetition rate of 140 kHz. This new upgrade of the technology now refers to the sensor as the Chiroptera-4X. The standard flying height of 400 m above ground level was executed for this flight and flight lines were planned with 30% overlap.

2.3 Time of Flight Conditions

The meteorological conditions during and prior to the topo-bathymetric lidar survey are important factors in successful data collection. As the bathymetric lidar sensor is limited by water clarity, windy conditions have the potential to stir up any fine sediments in the water and prevent laser penetration. Rain or fog are not suitable

for lidar collection, and sun reflecting off the water (sun glint) must also be factored in for the collection of aerial photographs. Before each lidar survey, weather forecasts from four web applications are monitored: the Environment and Climate Change Canada (ECCC) public weather forecast (http://weather.gc.ca/), ECCC's Marine Forecast (http://weather.gc.ca/marine/index_e.html), SpotWx (www.spotwx.com) in which a user can enter a precise location and choose from several forecasting models of varying resolutions and lengths, and lastly, a customized ECCC forecast delivered to AGRG every 8 hours. Each of these tools has strengths and weaknesses and it was through monitoring all four that a successful lidar mission was achieved. For example, the customized ECCC forecast was the only tool that provided an hourly fog prediction. However, the SpotWx graphical interface proved superior for wind monitoring. Only the ECCC public forecast provided Weather Warnings that were broadcast in real-time, such as thunderstorms, and the marine forecast provided the only information for offshore conditions. All these websites were monitored to choose a favorable day for the survey.

A weather station installed by AGRG on the shore of Megs Cove on Cape John provided local weather data for the lidar survey (Figure 2.4). Moderate Northeast winds with no rainfall was recorded during the lidar survey timeframe. However, in the weeks leading up to the survey the amount of rainfall events were significant and water levels in the river were much higher than in the summer during the ground-truth campaigns. The increased rainfall also resulted in the water becoming darker and less transparent than during the more ideal planned survey time in August compared to October.

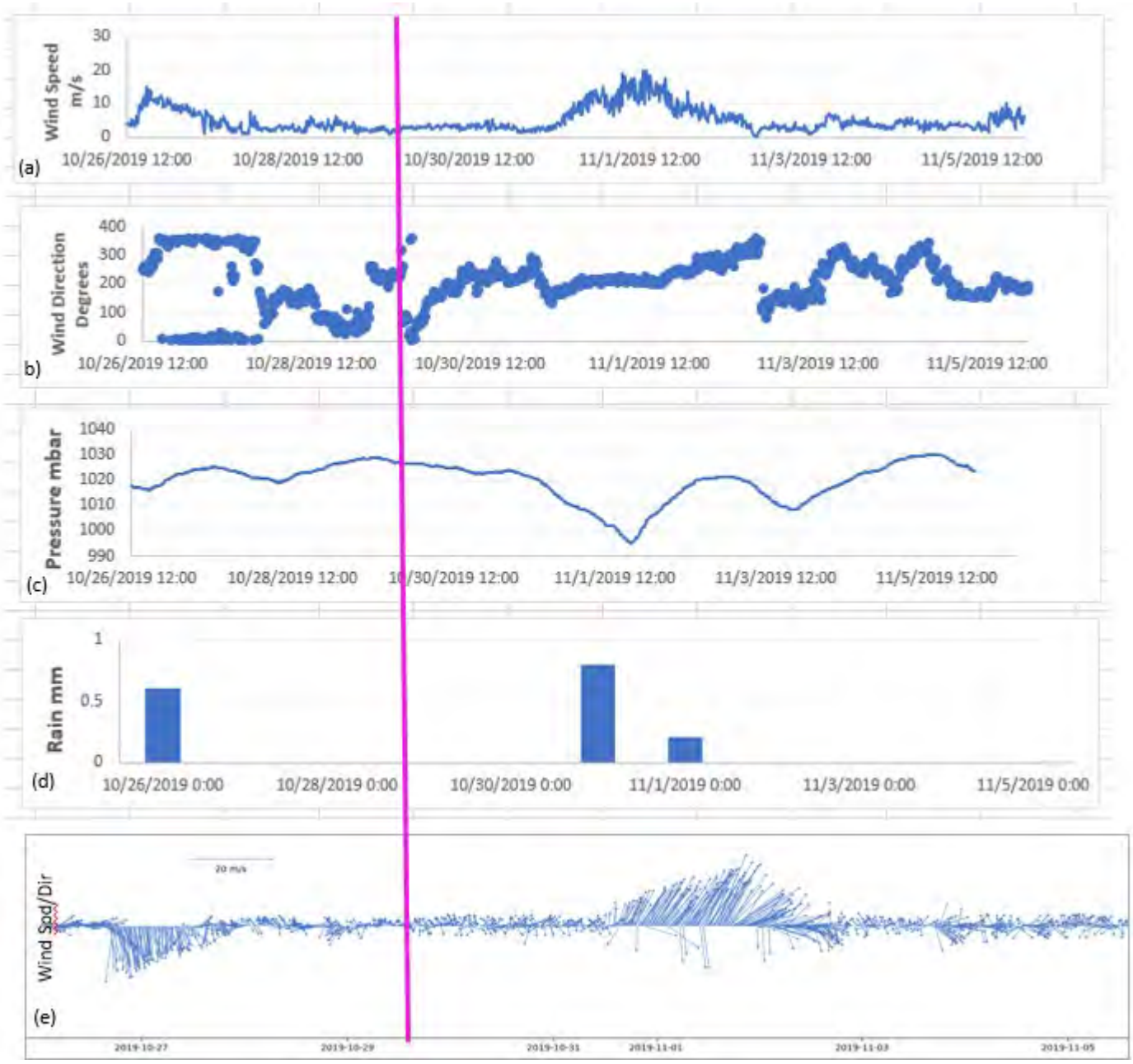

Figure 2.4 Cape John Metrological data during the lidar survey. (a) Wind speed and (b) direction collected at the AGRG-NSCC weather station between 26th Oct – 5th Nov 2019 at 15 min intervals. Panel (c) pressure recorded at the station in mbar(d) rainfall in mm and (e) shows a vector plot of the wind, where the arrows point in the direction the wind is blowing. The pink solid line represents the time of the survey.

2.4 Ground Truth Data Collection

Ground truthing data collection is an important aspect of topo-bathymetric lidar surveys. Months prior to the lidar survey, field work was carried to collect a wide range of information. Table 1 summarizes the field work activities for the River John in 2019-2020.

Date	Secchi (Y or -)	Depth (see caption for options)	Hobo underwater temperature and pressure sensors	Hard Surface GPS (Y or -)	RiverRay Flow ADCP (Y or -)	Water temperature	Flow	Water samples
31-Jul	Y	P	PS	Y	Y			Y
1-Aug		P			Y			
20-Aug		P	PS		Y	Y	EM	
21-Aug		P		Y		Y	EM	
6-Sep		P	PS				EM	
26-Sep							EM	
21-Oct	Y						EM	
Feb 20, 2020				Y				

Table 1: River John ground truth data summary. GPS Column: Depth Column: P=GPS antenna threaded onto the large pole for direct bottom elevation measurement, Y- yes. PS- Pressure sensor installed. Flow column: EM is Valeport Electromagnetic flow meter.

Two pressure sensors were deployed, one near an old iron railway bridge in the tidal influence zone and the another one attached to the crib work near an old water pipe in Welsford (crib work laid out in early 1900's to carry water to the train station) on July 31 and Aug 20, 2019 respectively but data from the loggers were only used from Sep 6 after the pressure sensor at the iron bridge was redeployed (Figure 2.5). Over the field work season water levels at these locations were taken using GS 14 Global Navigation Satellite System (GNSS) (Figure 2.5(a) and (d)). Figure 2.6 shows the compensated pressure sensor information at both these locations. Water samples and Secchi depth measurements were collected for information on water clarity. The riverbed elevation at various locations was measured using a pole which had the Real Time Kinematics Global Positioning System (RTK – GPS) threaded on top.

Currents near the tidal inlet were measured using a Teledyne RiverRay which is a small towed vessel containing a downward looking 600 kHz Acoustic Doppler Current Profiler (ADCP) that measures the cross-sectional depth and flow of the channel. Multiple transects were collected using the RiverRay towed behind a Kayak (Figure2.5). Several flow measurements using Valeport EM model 801 were collected at the water pipe pressure sensor before and after Hurricane Dorian (September 7-8th, 2019).

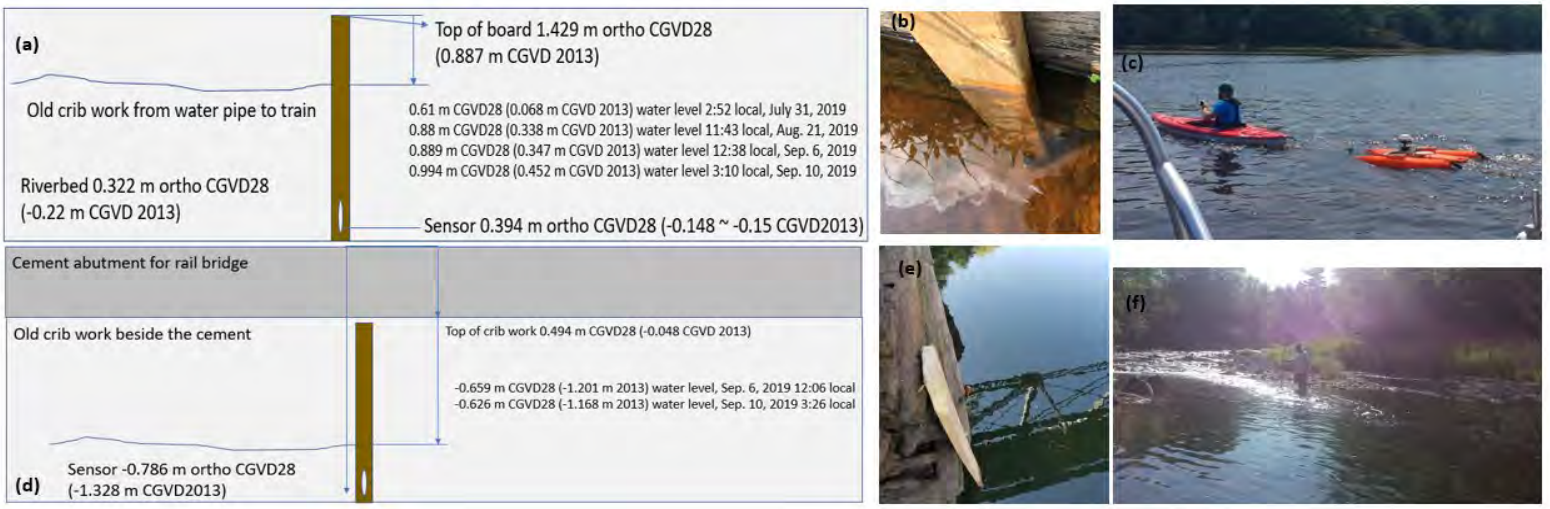

Figure 2.5 (a) Pressure sensor schematic upstream (b) Pressure sensor on a board attached to crib work near old water pipe (c) AGRG researchers conducting River Ray transect (d) Pressure sensor schematic downstream (e) Pressure sensor on a board attached to crib work to Iron bridge (f) Tim Webster collecting GPS transects.

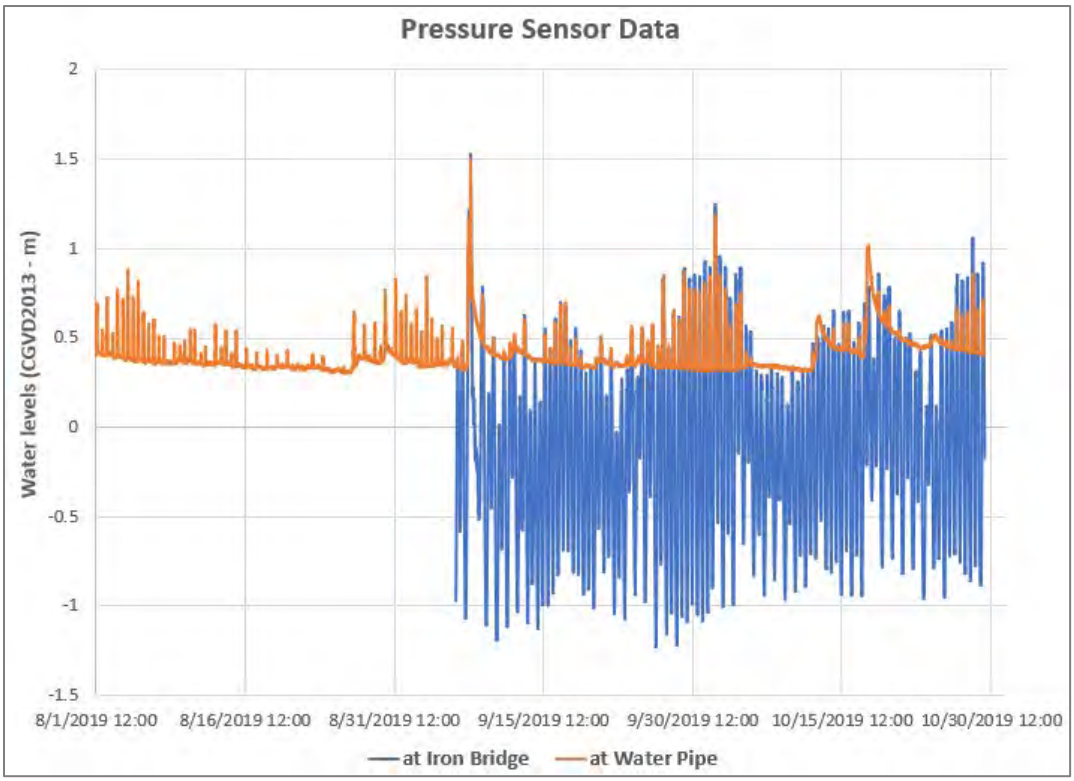

Figure 2.6 Data collected with Hobo pressure sensors at the Iron bridge and water pipe

A total of 828 points were collected using an RTK-GPS on hard surfaces, and in the river and floodplain (Figure 2.7). Near the mouth of the river where the water is deeper GPS points were collected with an antenna threaded on a painter's pole and depths were measured from the Boston Whaler. Upstream where the water is shallower cross section points were collected while crossing the river at various locations (Figure 2.5 (f)).

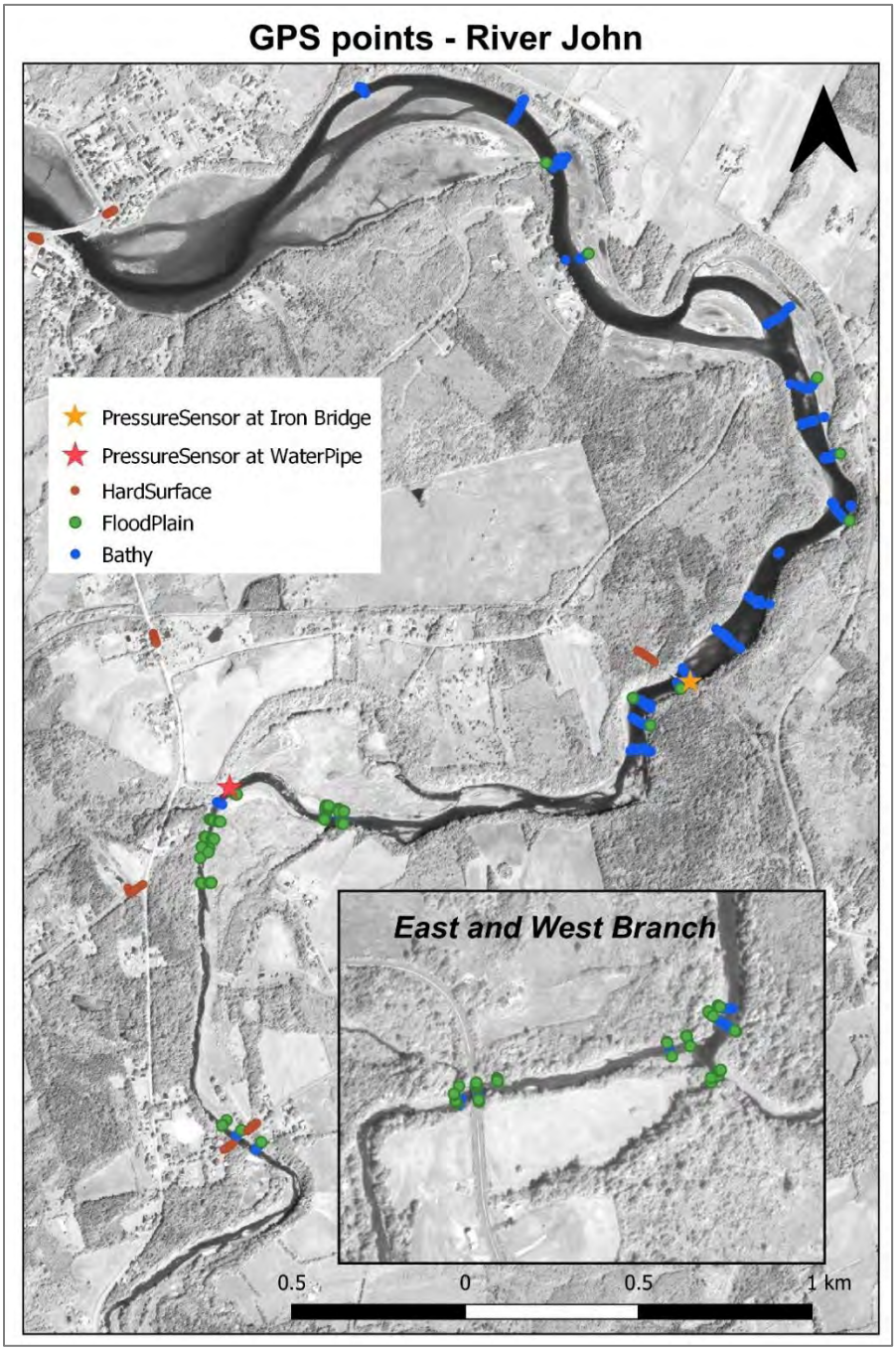

Figure 2.7 GPS points collected on hard surfaces, cross sections in the river and floodplain (background - World View image). Inset: GPS points collected where East and West branch meets.

2.5 Data Processing

2.5.1 Lidar Processing

GPS trajectory along with the data from the Inertial Motion Unit (IMU) was processed in Inertial Explorer software using the Nova Scotia Active Control Stations (NSACS) network as a base station. This post processed trajectory was linked to the laser returns and were georeferenced. Lidar Survey Studio (LSS) software accompanies the Chiroptera-4X sensor and was used to process the lidar waveforms into discrete points. These

data were then inspected to ensure there was sufficient overlap between flight lines (30%) and no gaps existed in the lidar coverage.

Using the new LSS software version 2.60.00 a better water surface was derived from the lidar returns of both the topo (NIR) and bathy (green) lasers. Initially processed data were broadly classified into land and bathymetry but typically needs to be refined. This refinement is generally carried out in TerraScan™ software after the LAS point data are tiled into 1 km blocks or any size depending on the point density and classified into standard bathymetric classes in Las 1.4 format (Figure 2.8). Before the refined classified LAS files can be read into ArcGIS, the water surface and bathy classes were changed into a lower class value as ArcMap doesn't recognize any classes beyond 30, then a variety of raster surfaces at a 1 m spatial resolution were produced.

Classification Value	Meaning
40	Bathymetric point (e.g., seafloor or riverbed; also known as submerged topography)
41	Water surface (sea/river/lake surface from bathymetric or topographicbathymetric lidar; distinct from Point Class 9, which is used in topographic-only lidar and only designates "water," not "water surface")
42	Derived water surface (synthetic water surface location used in computing refraction at water surface)
43	Submerged object, not otherwise specified (e.g., wreck, rock, submerged piling)
44	International Hydrographic Organization (IHO) S-57 object, not otherwise specified
45	No-bottom-found-at (bathymetric lidar point for which no detectable bottom return was received)
46-63	Reserved
64-255	User definable

Figure 2.8 Lidar point classification Codes and descriptions of bathymetric feature Las 1.4 standard.

2.5.2 Aerial photo processing

Images collected by the RCD30 (Figure 2.2 (d)) at 60 megapixels were processed and georeferenced using the aircraft trajectory in Agisoft PhotoScan Professional to produce a 5 cm Ground Sample Distance (GSD) orthophoto. A Digital Elevation Model (DEM) produced from the lidar data or a Digital Surface Model (DSM) derived from the photos is required in the orthorectification process along with the linked aircraft trajectory to the photo events by the GPS time tags.

2.6 Hydrodynamic modelling

MIKE 11 and 21 developed by the Danish Hydraulic Institute (DHI) is depth averaged hydrodynamic modelling system based on the incompressible Reynolds averaged Navier – Stokes equations was used to produce flood maps for River John.

The usefulness of topo-bathymetric lidar in riverine modelling were tested in both a simple one-dimension modelling environment (MIKE-11) and a more computationally intensive two-dimensional model (MIKE-21). The DHI MIKE hydrodynamic modelling suite was used to simulate three inundation events, i) a significant historical event, the September 8, 2019 Hurricane Dorian, that was observed with several pressure gauges, ii) a future climate change 1:100 year event using the RCP 8.5 rainfall guideline of 107 mm in a 24 hour period (WSP, 2020), and iii) a forced flooding event that increased the magnitude of the 1:100 year event by a factor of three (321 mm) to produce significant floodplain inundation. The influence of the tide was represented in each river model by incorporating simulated water levels from the developed Mike21 deep water model for the Dorian event. Model inputs and parameters are discussed within the following sections.

2.6.1 2D model

A two-dimensional hydrodynamic model was required to map flooding caused by the overtopping of riverbanks represented in the scenarios discussed above. The Mike21 software package was used to calculate depth averaged two-dimensional hydrodynamics over a DEM of the earth's surface generated from high-resolution topo-bathymetric lidar. A variety of sources and resolutions of topography and bathymetry data were compiled (Table 2) to generate a high-quality bathymetry grid in order to complete the flow model for the two domains: domain 1) deep water and estuary 2) river. Elevation models were computed using the spline technique (Wahba, 1990) within the ESRI ArcGIS software package to generate a low-resolution 15 m grid for the deep-water area and estuary (Domain 1) and high-resolution 3 m grid for river (Domain 2) (Figure 2.9). Topographic data were restricted to a maximum elevation of 10 m in Domain 1 and 100 m in Domain 2 to limit the number of grid cells used in the simulations while ensuring that inland areas were well represented and susceptible to maximum inundation levels for all modelled storm surge events.

Domain	Provider	Method	Offset applied/ notes	Native Resolution	Year
River & floodplain	AGRG	Topobathy lidar survey using Chiropter-4X sensor	Ellipsoidal heights to CGVD 2013 using CGG model	1 m	2019
Topo Dem	GeoNOVA	Topo survey	Ellipsoidal heights to CGVD 2013 using CGG model	1 m	2018
Topo DEM for Brule point and Marshville	AGRG	Topo survey	CGVD 1928 to CGVD 2013 using CGG	1 m	2011
Deepwater	CHS	CZMIL	CD to CGVD 2013 using CVD	Variable Delivered 5 m	2017
Deepwater	CHS	ENC 376161 - Chart 4405	CD to CGVD 2013 using CVD	Variable	

Table 2 Bathymetric and topographic data sources, resolution, method and offset applied to convert from CD, CGVD 1928 to CGVD 2013. CGG – Canadian Gravimetric Geoid model for CGVD2013.

Ellipsoidal heights were converted into Canadian Geodetic Vertical Datum (CGVD) of 2013 using the Canadian Gravimetric Geoid model (CGG) from the Geodetic Survey of Canada, part of Natural Resources Canada. Data from the Canadian Hydrographic Services (CHS) was in Chart Datum (CD which is Lower Low Water Large Tide (LLWLT)) was converted to CGVD 2013 using the Continuous Vertical Datum (CVD) from CHS.

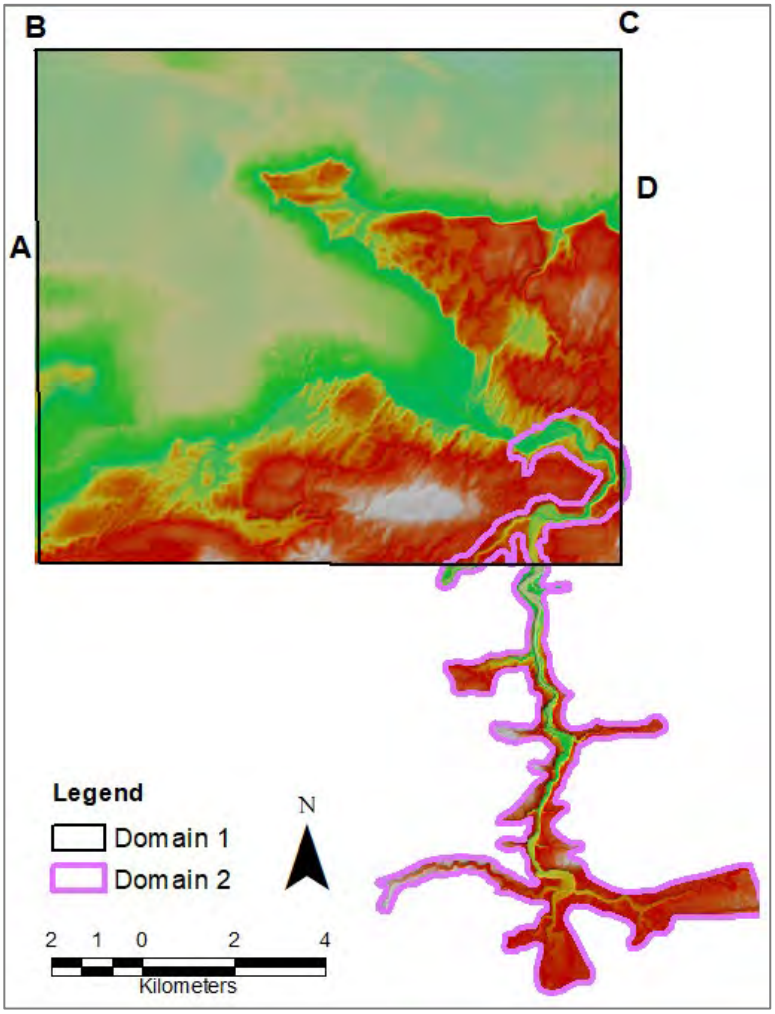

Figure 2.9 Domain 1 Deepwater and estuary along with Cape John gridded at 15 m low resolution. Domain 2 River and floodplains gridded at 3 m high resolution. Open water boundaries for tides on West AB, North BC, and East CD

As the hydrodynamic model was driven by tidal predictions along the open water boundaries in the west (AB), east (CD) and north (BC) for Domain 1 and mouth of the river for Domain 2 using profile series files in MIKE generated by the data from WebTide (Dupont et al., 2002) for the time frame of Hurricane Dorian Aug 24th to Sep 10th, 2019. Tidal predictions from WebTide were extracted at ABCD and at the pressure senor installed by AGRG in Skinners Cove. To compute the residuals of Dorian (Figure 2.10) at Skinners Cove the WebTide predictions were subtracted with the tide gauge data after converting the water levels to CGVD 2013 using an offset of -0.462 obtained from the CVD at the location. These residuals were added to the tidal predictions at the boundary corners after converting to CGVD 2013 using an offset of -0.525m at A, -0.511m at B, -0.430m at C and -0.448m at D from Mean Sea Level (MSL), were utilized for the simulation.

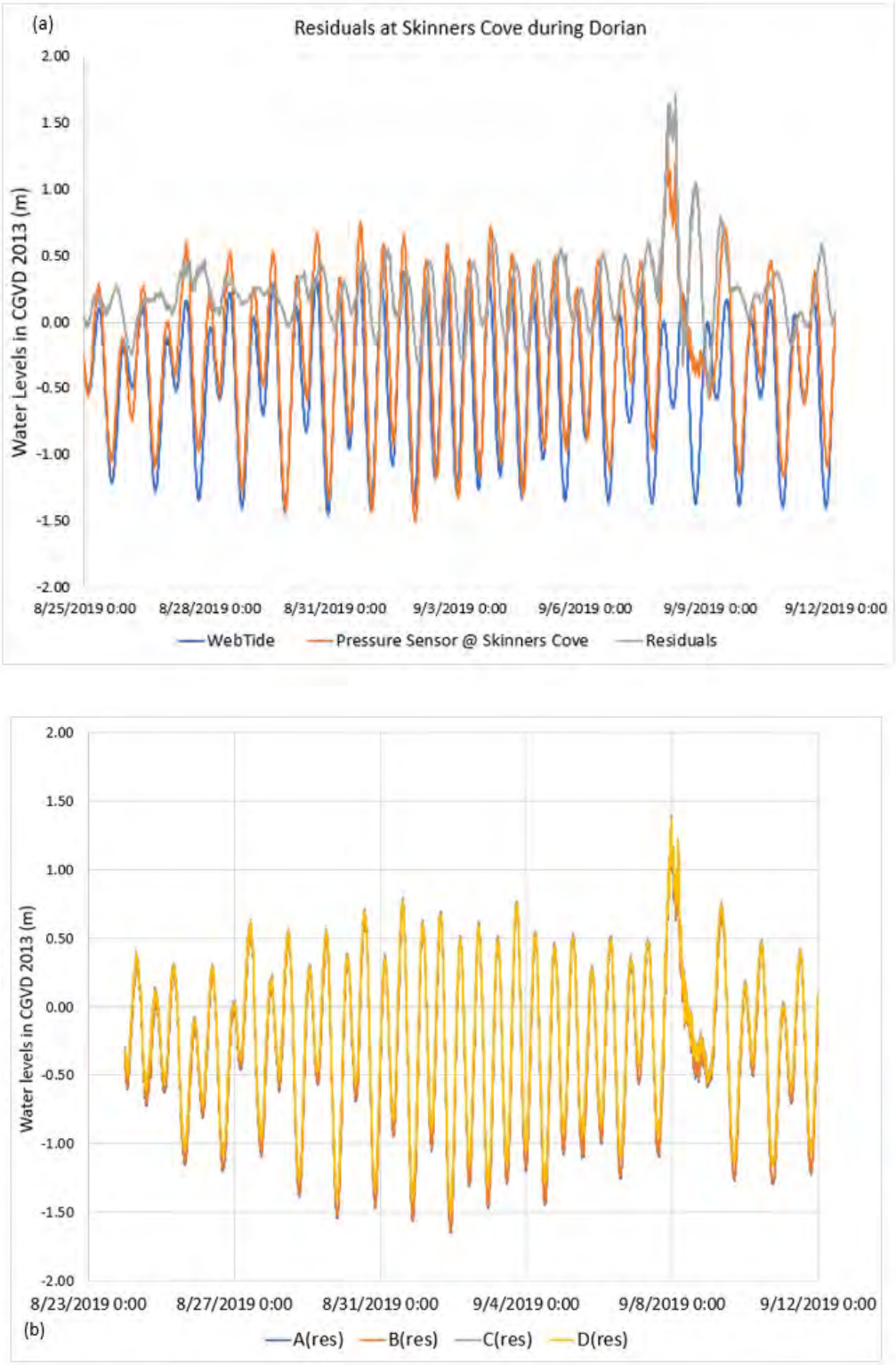

Figure 2.10 (a) Calculated residuals at Skinner Cove (b) Residuals at boundaries A,B,C, and D applied to the model

Results were extracted from the deep-water model at the Sunrise Trail (Highway 6) bridge and were used as the tidal input to run the river model. The two-dimensional model effectively calculated the transfer of water between adjacent hydrologically connected cells within the model domain (Figure 2.11).

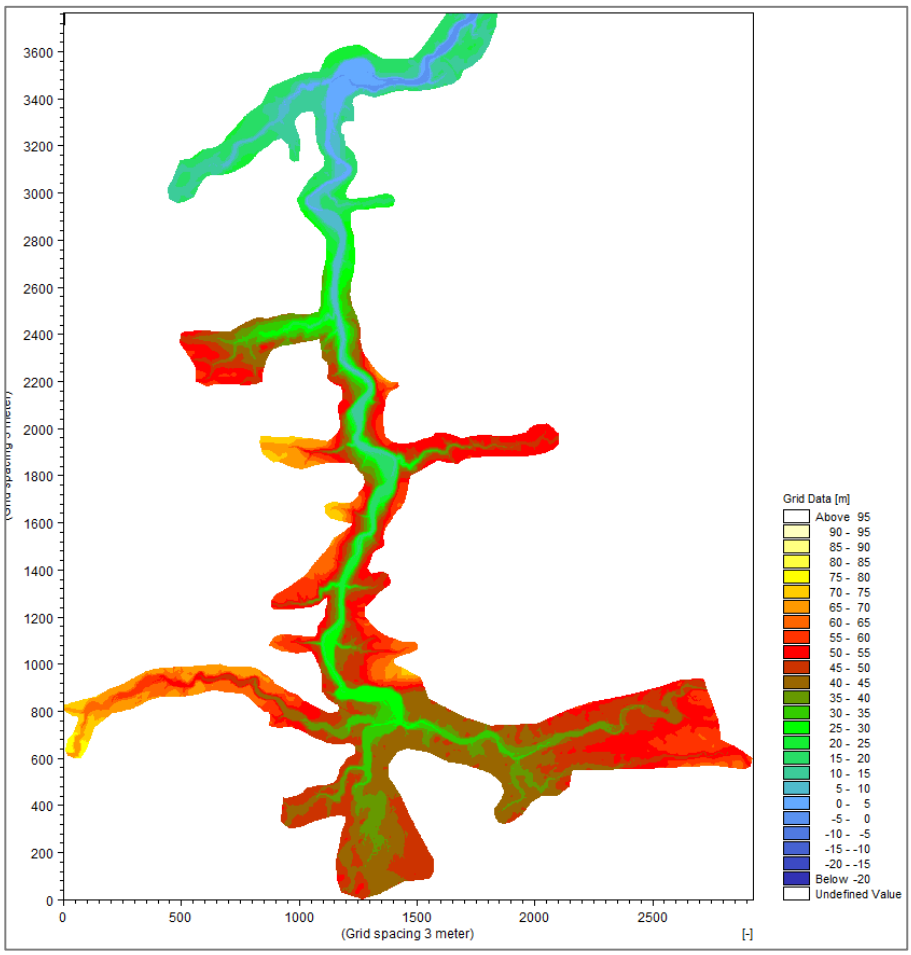

Figure 2.11 Mike21 River John model domain with ineligible flood cells removed.

2.6.2 1D model

The geomorphology of a study area is the most import factor for several hydrodynamic model components. While stream networks and watershed boundaries can be defined using standard quality elevation data, the accurate representation of river channel and floodplain geometries require high quality elevation data from sources such as TB-lidar. A cohesive elevation model was developed for River John and surrounding watersheds by merging the NSCC-AGRG collected 1 m lidar DEM with 25 m resolution elevation data from the Shuttle Radar Topography Mission (SRTM). The 25 m data were required to fully represent and calculate the River John watershed extents using a suite of hydro tools within the ESRI ArcMap 10 software package. The DEM was appropriately prepared by lowering elevation values where bridges existed to ensure proper drainage characteristics between adjacent cells. In the correction process, each structure was removed from the DEM and the lowest surrounding elevation value was used to fill the void. The tools were used to simulate theoretical drainage between adjacent cells based on elevation differences to form watershed boundaries and river networks based on accumulated flow calculations (Figure 2.12).

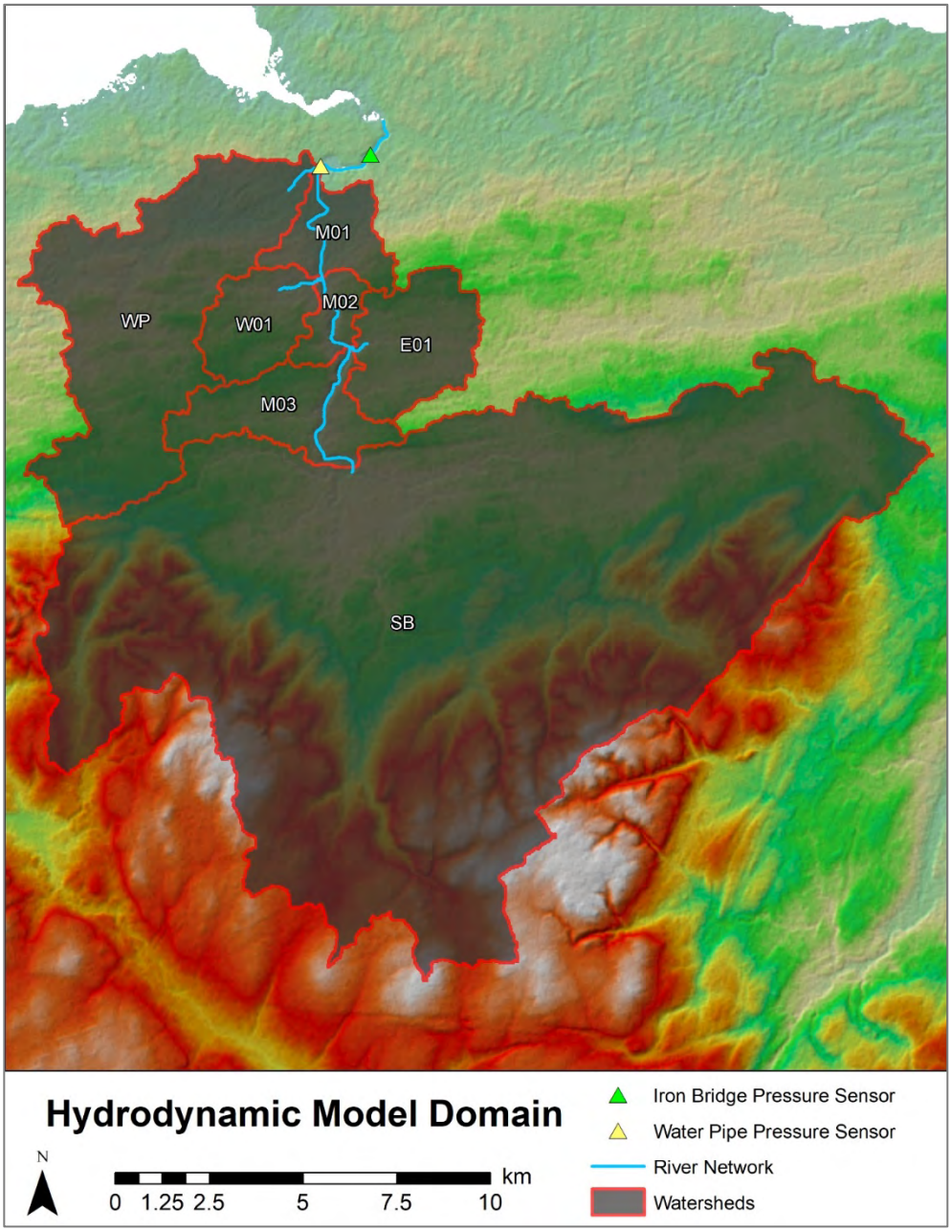

Figure 2.12 Hybrid digital elevation model of the River John watershed generated using 25 m resolution SRTM elevation data and 1 m resolution lidar data.

The Mike11HD model required accurate stream and floodplain topography to simulate the flow of water through the system. The river network was sectioned into unique branches with length (chainage) measured in meters. Each branch was then linked with its appropriate catchment in order to create a stable network input for simulations. Mike11HD uses the conservation of momentum principle to calculate flow at defined river cross-sections in order to transfer flow between cross-sectional distances. Cross-sections were manually digitized across river branches and floodplains perpendicular to the direction of flow. Cross-sections were roughly spaced at 300 m intervals along river branches while ensuring that a cross-section was drawn at the

start and end chainage of each river branch. Cross-section width was dependent on topography and was ensured to capture potential floodplains during significant flooding events (Figure 2.13). Elevation was extracted from the hybrid DEM and applied to each cross-section. Conveyance and water levels were calculated for each of the one-dimensional cross-sections based on theoretical water elevation within the cross-section at 1 cm increments. Cross-section topography and conveyance potentials were stored within the final cross-section input file for hydrodynamic (HD) simulations (Figure 2.14). Additional cross-sections were interpolated along the river network to establish a 100 m minimize distance between adjacent cross-sections to improve model stability (Figure 2.15).

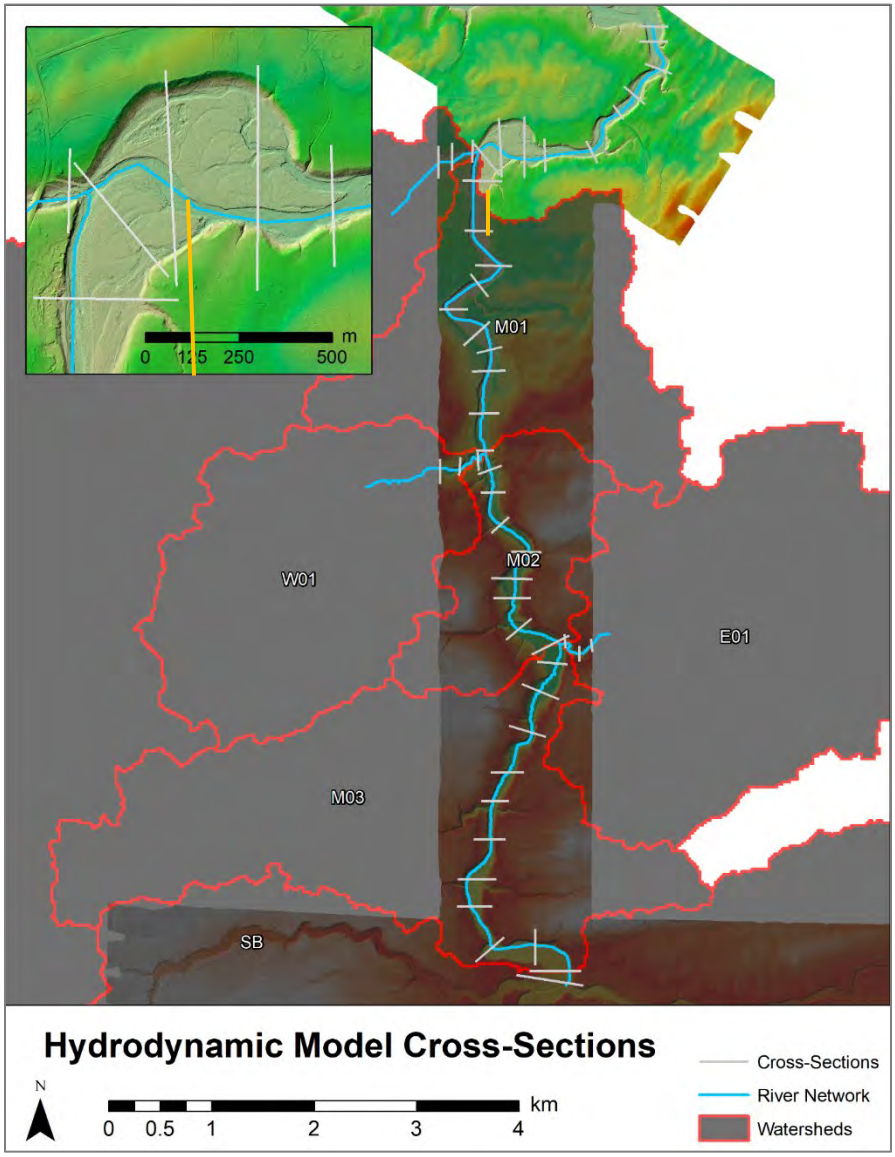

Figure 2.13 Delineated cross-sections extending from the river to beyond floodplains used to calculate the conveyance of water within the model domain. The highlighted eastern cross-section within the inset map is presented in detail below.

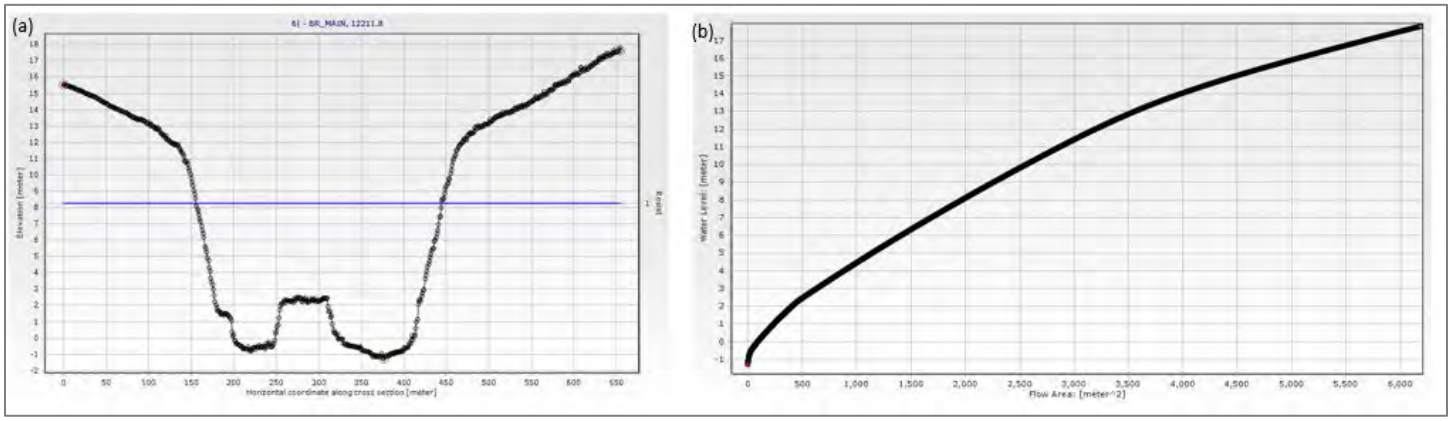

Figure 2.14. (a) River John cross-section oriented perpendicular to flow. Elevation data along the length of the cross-section were extracted from the topo-bathymetric lidar DEM. The minimum possible water level corresponded to the minimum elevation on the well-defined main branch of the river (red dot); (b) Potential conveyance was calculated based on water level increments within the possible flood area at 1 cm vertical increments.

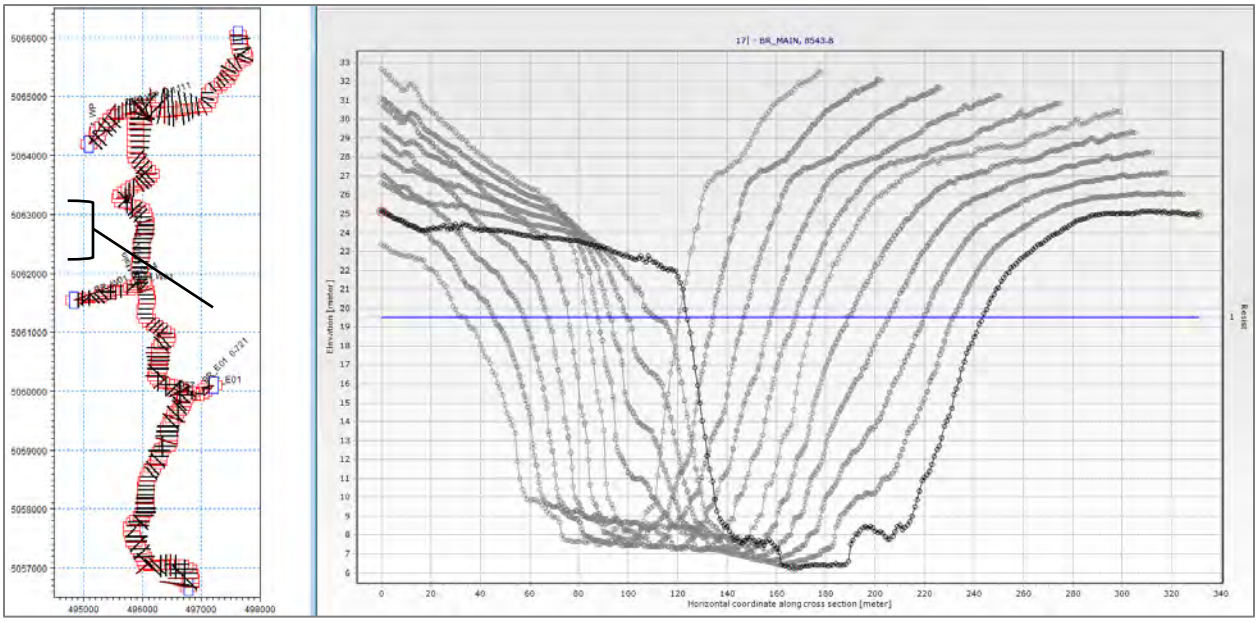

Figure 2.15. Mike11 river network with cross-section locations highlighted in red. Ten 2-D cross-sections are emphasized to demonstrate the smooth bed elevation changes in the valley south of the W01 watershed confluence.

The River John rainfall runoff model was driven by a Rainfall Dependent Inflow and Infiltration model (RDII) within the Mike11 software suite, by DHI. The rainfall runoff model is a generalized watershed model that simulates the discharge of water by quantifying routing times and storage zone capacities. The volume of water that exceeded the storage capacity of each watershed was routed into the river system at the defined cross-section locations. The River John system was defined as a main branch that ran 11, 485 m from south to north. The main branch was met by 3 ancillary branches, the Water Pipe branch (BR_WP), the major western branch (BR_W01) and major eastern branch (BR_E01). Watershed loadings were linked to the river branches using start and end distances (chainages). Each ancillary branch and chainages along the main branch, including the major southern watershed (S01) were linked to the river network as described in Table 3. With linkages

complete, the model was ready to be calibrated and produce flood simulations.

Watershed Name	Watershed Area (km^2)	River Branch Name	Upstream Connection Chainage (m)	Downstream Connection Chainage (m)
M01	6.225	BR_MAIN	7644	11485
M02	3.176	BR_MAIN	4957	7644
M03	10.317	BR_MAIN	130	4957
WP	36.8	BR_WP	0	1111
W01	7.191	BR_W01	0	1544
E01	10.514	BR_E01	0	721
S01	204.504	BR_MAIN	0	130

Table 3 River John linkages between major watersheds and river branch chainages.

The most significant input to the River John one-dimensional model was rainfall. The majority of other input parameters control the volume and timing of water as it moves through the river system. The standard practice is to establish these timing parameters using an iterative calibration process over an observed event. The River John system was gauged by NSCC-AGRG in three locations. A weather station was established in Cape John to provide wind, pressure, temperature, and precipitation data. The river was gauged using submerged pressure sensors in two locations, the Iron Bridge, and the Water Pipe. Pressure sensor locations were measured using survey grade GNSS receivers to establish their elevation relative to the CGVD2013. Pressure sensor depth readings were barometrically compensated using the weather station barometer to establish an accurate depth of water above the sensor, depths were then converted to CGVD2013 surface elevations. This method was used to generate river surface elevation timeseries at 15-minute intervals for 2019 which matched the duration and interval of the meteorological timeseries produced by the weather station. The River John one-dimensional model was calibrated using observed precipitation for the 2019 Hurricane Dorian event where elevated levels were observed in River John caused by both marine storm surge and freshwater input.

Marine input to the one-dimensional model was simulated by adjusting the water level at most downstream cross-section of the River John model. Water level elevations were extracted from a deep-water two-dimensional Mike21 model designed to simulate storm surge generated by the Hurricane Dorian event. Extracted elevations were used to transfer the marine model results to the cross-section ensuring that water level and timing were preserved. The freshwater input was modelled by simulating rainfall intensities over the watershed catchment areas and adjusting storage capacities and routing times until model results closely matched pressure sensor observations at the Water Pipe and Iron Bridge locations (Figure 2.16).

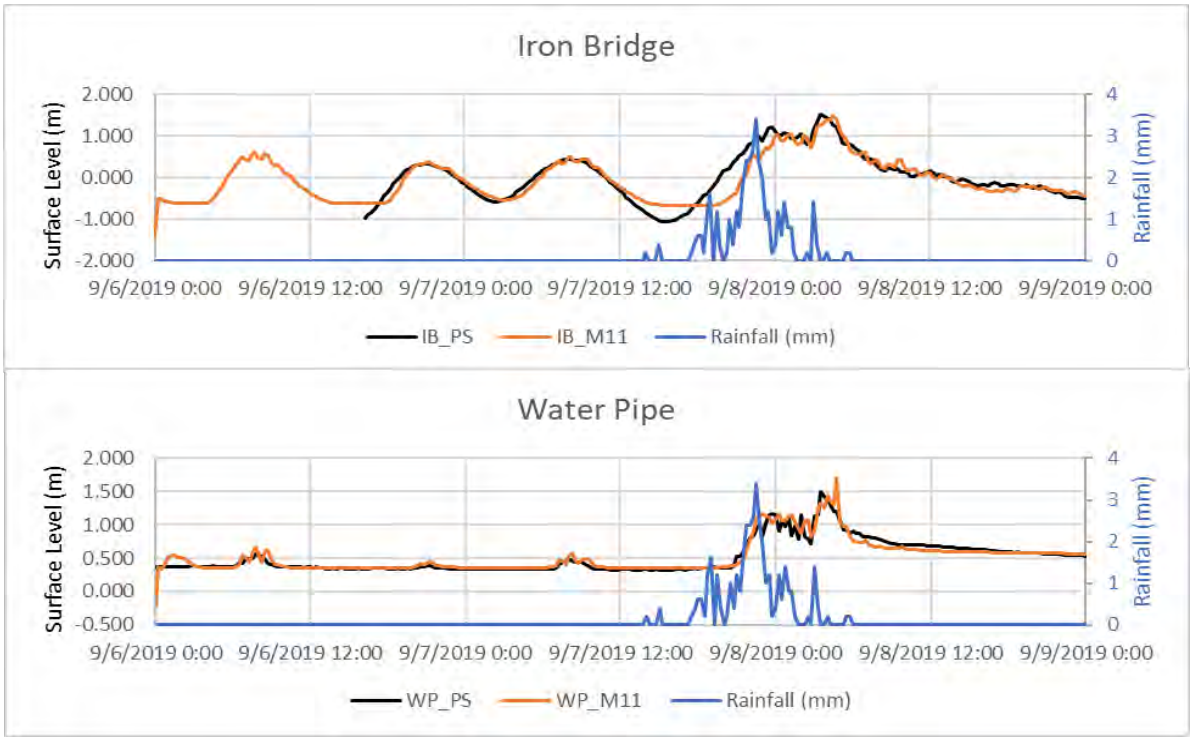

Figure 2.16 Validation of the Mike-11 simulation of Hurricane Dorian comparing the water level observed at the Iron Bridge pressure sensor (IB_PS) against Mike11 simulated levels (IB_M11) and the Water Pipe pressure sensor (WP_PS) against simulation results (WP_M11) with rainfall imposed.

Once calibrated, the Mike11 model was used to generate surface level predictions for two additional events defined as: 1) the future climate change 1:100 year event using the RCP 8.5 rainfall guideline of 107 mm in a 24 hour period (WSP, 2020), and 2) a forced flooding event that increased the magnitude of the 1:100 year event by a factor of three (Figure 2.17).

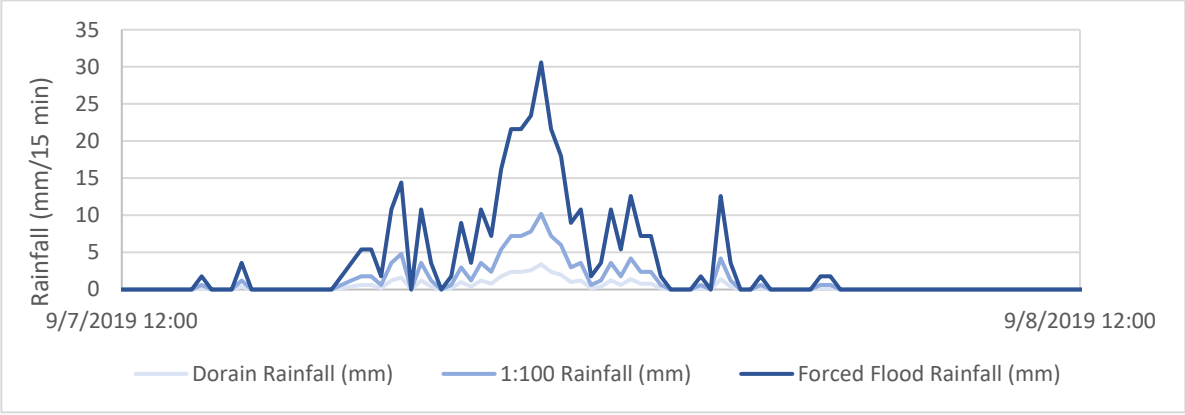

Figure 2.17 Rainfall intensity comparison between the observed Hurricane Dorian event, the 1:100-year future climate change event and a synthetic rainfall scenario designed to cause major flooding.

Each model scenario successfully routed rainwater from the catchments, to the river network through the lidar derived cross-sections to generate surface level and velocity predictions along the River John model domain and were found to be stable under extreme rainfall scenarios (Figure 2.18).

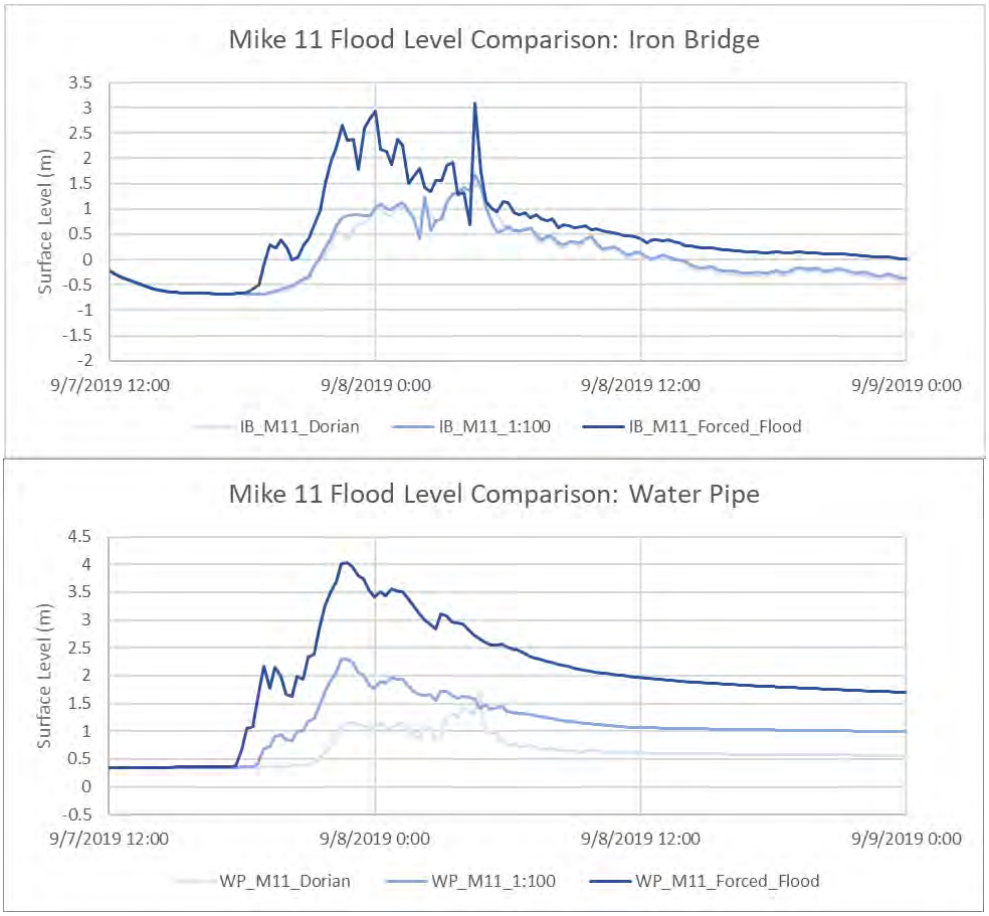

Figure 2.18. Mike11 simulated surface levels (CGVD2013) at the Iron Bridge and Water Pipe calibration cross-sections under observed Hurricane Dorian, climate change 1:100 year, and extreme rainfall levels to force floodplain inundation.

While the one-dimensional model is an excellent tool for simulating the response of catchments and river networks to rainfall events it is unable to accurately represent flooding between cross-sections and poorly captures the distribution of water on complex floodplains. To solve these shortcomings, the Mike11 model was linked with a two-dimensional Mike21 river model that was designed to utilize the high-resolution lidar data to accurately represent the geomorphology of River John and surrounding floodplains.

3 Results

This section describes the lidar validation and map products, and the modelling validation and simulation results.

3.1 Lidar Results

A Digital Elevation Model (DEM) and Digital Surface Model (DSM) (Figure 3.1) at 1 m resolution were gridded using ArcMap after reclassing the refined las points whose heights are in ellipsoidal were converted to CGVD 2013 using the CGG model. Trajectory had been processed with a base station 30km away as the one nearest

(Tata) was moved and has not been updated. There were some minor issues with the flight line overlap which was rectified by a blending tool developed by AGRG researcher which required separating odd and even flight lines data points and feeding the obtained rasters through the tool to produce a flight line adjusted DEM and DSM. Lidar penetration in River John was successful except near mouth of the river and east and west branch congregate where the water was darker. These rasters are generally void filled. An intensity raster was produced from the topo scanner classified las points along with the bathy points from the bathy scanner (Figure 3.2).

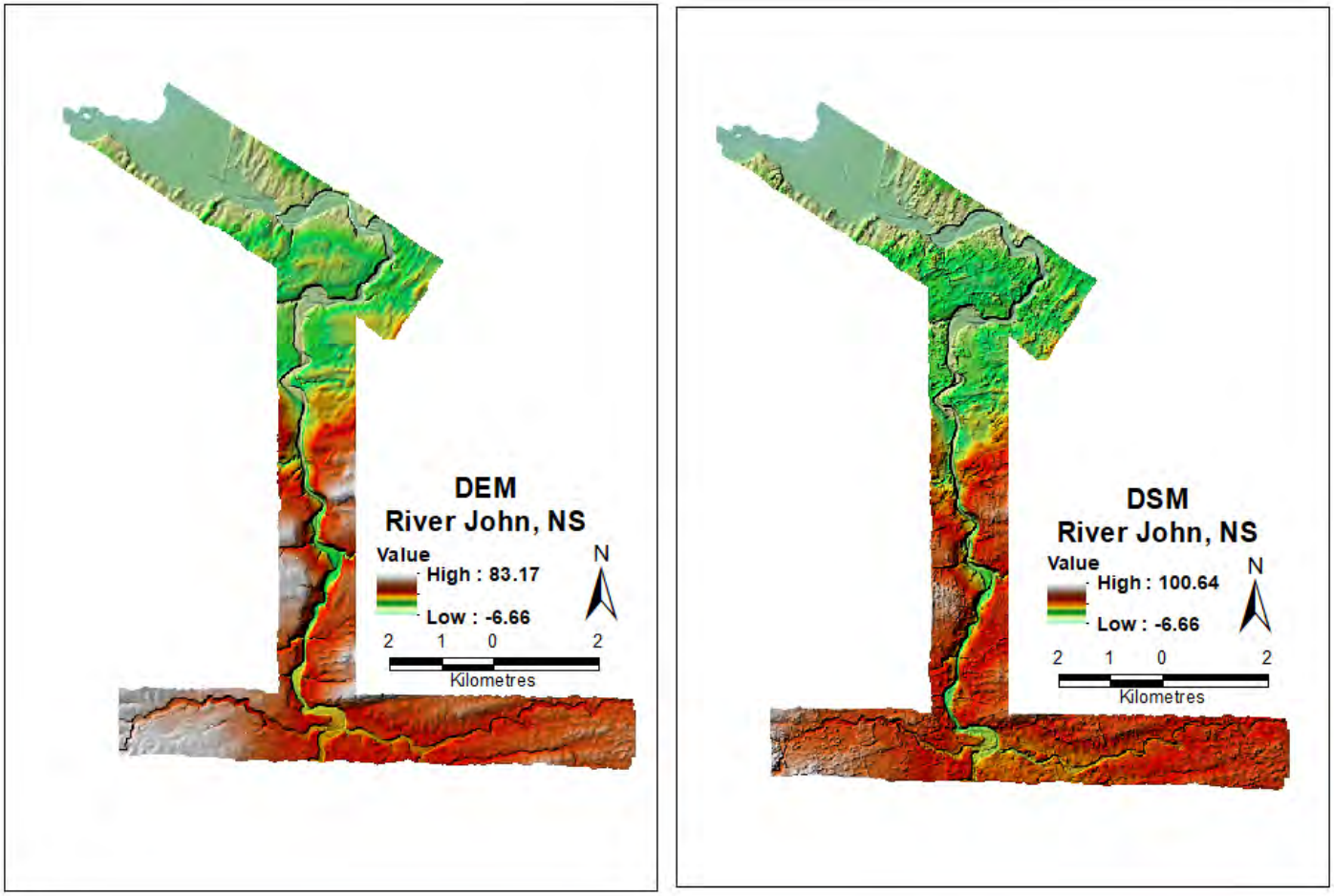

Figure 3.1 DEM and DSM at 1m resolution for River John in CGVD 2013.

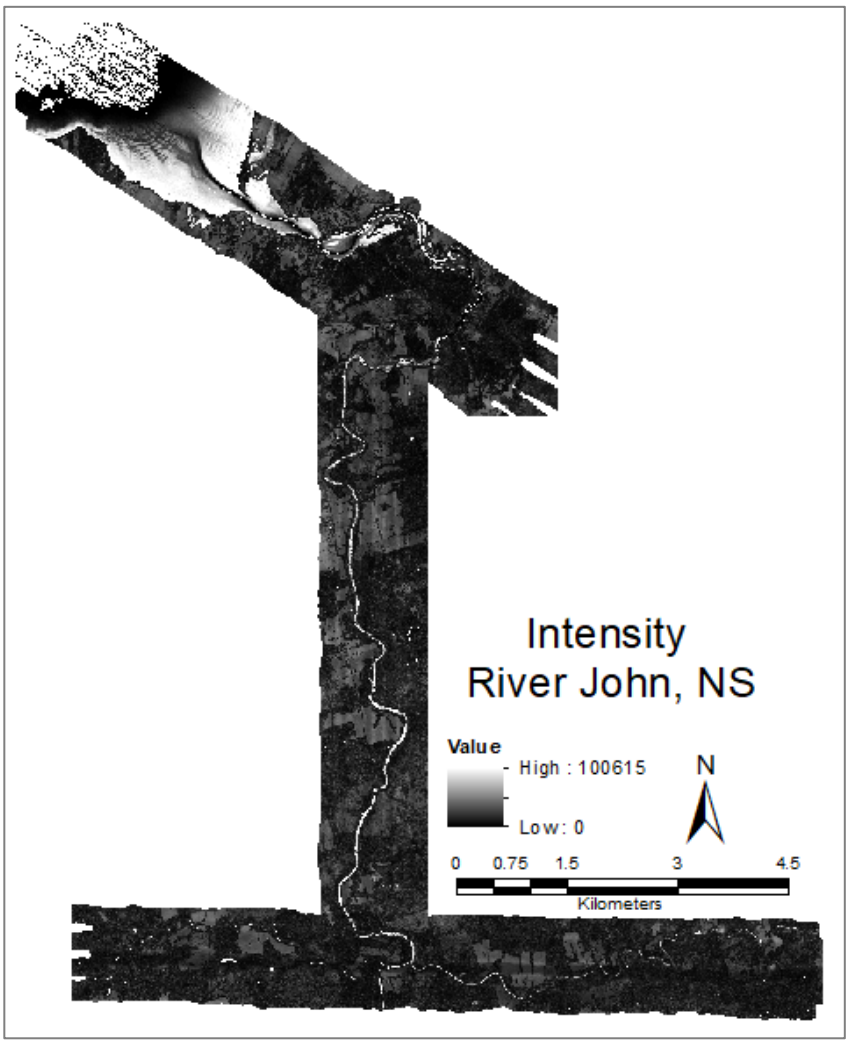

Figure 3.2 Intensity at 1m resolution.

3.2 Air photos

The orthophoto mosaic of 5 cm resolution consists of four bands (RGB + NIR) and provides insight into land use, water clarity, bottom type, wave action, and shoreline morphology (Figure 3.3).

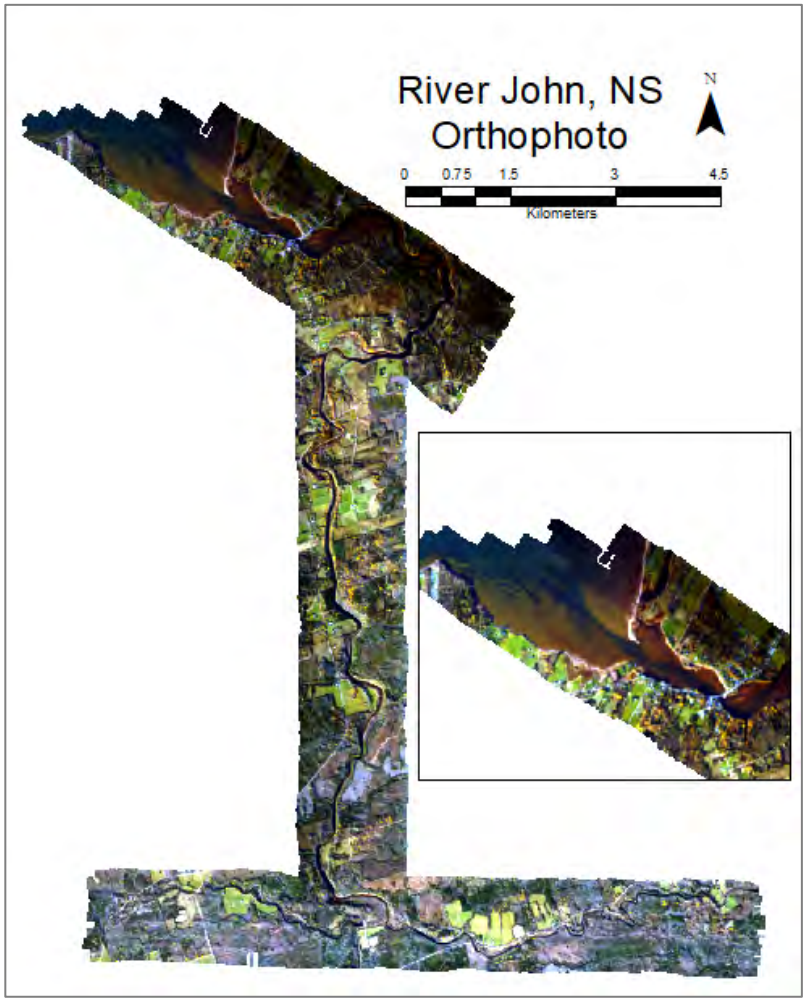

Figure 3.3 Orthophoto at 5cm resolution, inset – John Bay.

3.3 Submerged vegetation classification

A method for mapping eelgrass in bays using the topo-bathymetric lidar data and orthophotos was described in Webster et al. (2016), using this method for the River John survey, eelgrass beds along with spartina salt marsh vegetation were mapped and used as a bed roughness measure in the modelling (Figure 3.4).

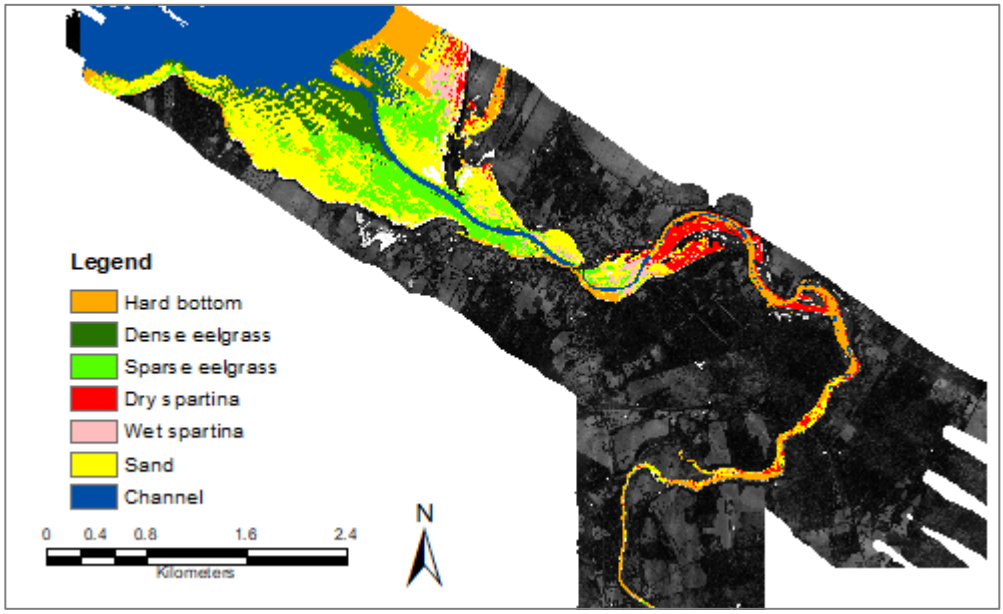

Figure 3.4 Submerged Vegetation classification for the River John estuary

3.4 Hydrodynamic modelling results

The one-dimensional hydrodynamic model was linked to the two-dimensional hydrodynamic model using the MikeFlood software package. The linkage allowed for the transfer of rainfall and stream level data calculated within the Mike11 model to be applied to the domain of the Mike21 model and vise-versa. The result was a model that was capable of accurately routing water between cross-sections and onto complex floodplains by transferring the momentum and level calculations to the two-dimensional elevation model. The result of the combined model are simulated water levels and velocities both within the river channel and the surrounding floodplains (Figure 3.5).

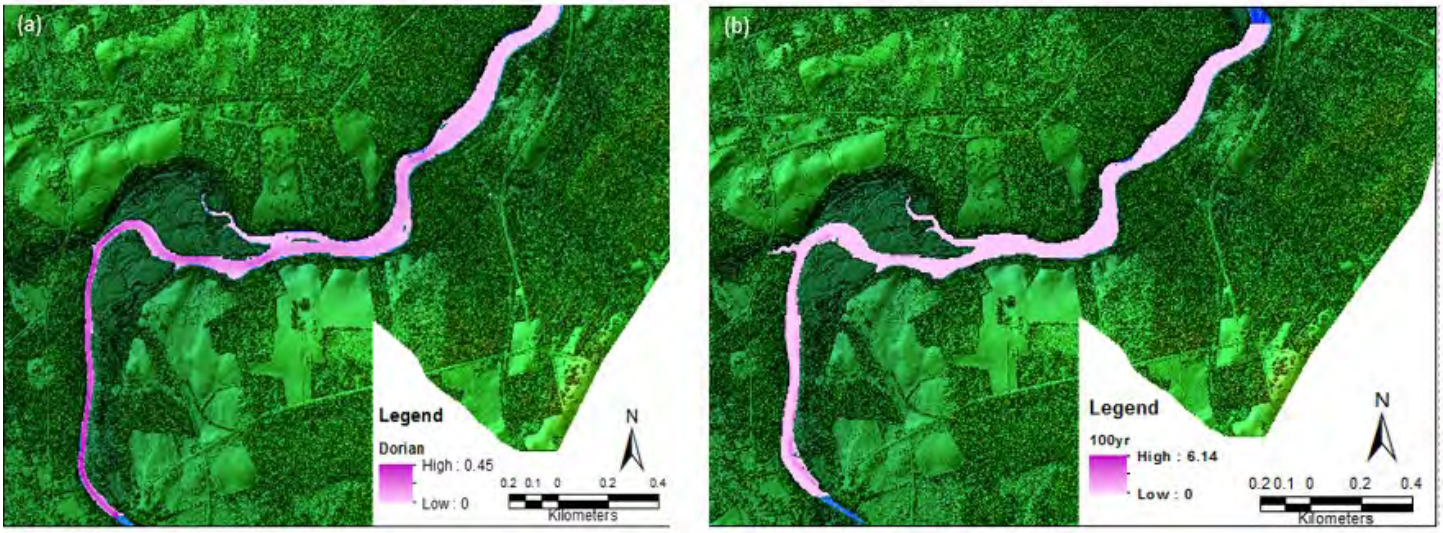

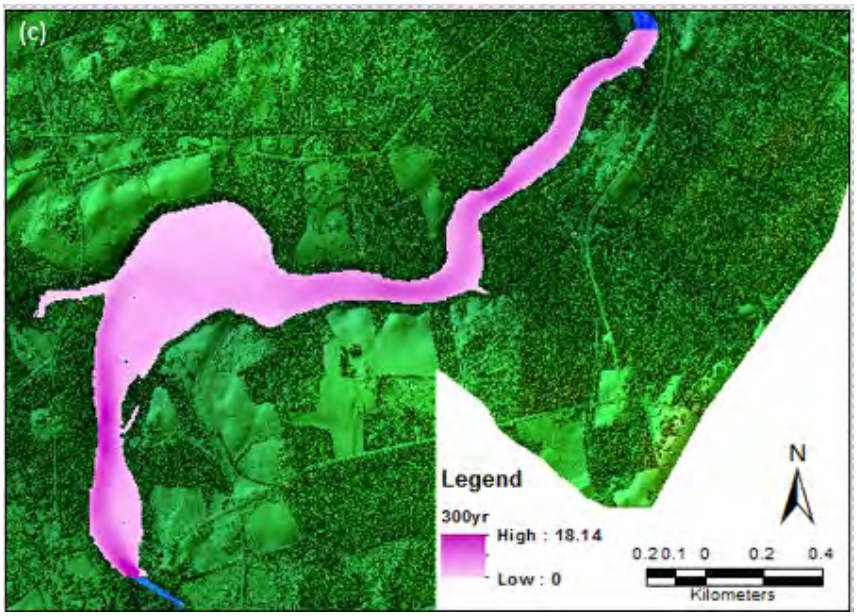

Figure 3.5 Simulated event to flood the entire floodplain. (a) Flood Hazard map (Depth X Velocity) for Dorian event (b) Flood Hazard map for future climate change 1:100 year event using the RCP 8.5 rainfall (c) Flood Hazard map for flooding event that increased the magnitude of the 1:100 year event by a factor of three.

3.5 Validation

3.5.1 Lidar Validation

To validate topographic lidar returns on areas of hard and flat surfaces, ground elevations were obtained using a Real Time Kinematic GPS with corrections transmitted via SmartNet network. These 59 GPS points were collected along roads, bridges and few landmarks in the study site. The elevation difference (Dz) was calculated by extracting the Z from the DEM at the points and subtracting these from the GPS elevations. A mean of 0.04 m with a standard deviation of ± 0.06m (Table 4) shows that the topographic lidar points validate within the specifications of the system.

For bathymetric lidar validation several GPS transects were collected from the boat in deeper water and manual crossings in shallow waters. A total of 828 points were collected of which 150 points on floodplain and outcrops along the banks of the river and 678 bathymetric points. Mean and standard deviation of calculated Dz with the elevations from the void and non-void filled rasters are given in Table 4.

GPS cover type	Raster	Total Points	Mean	SD
Topographic	Void filled and Non void filled	59	0.04	0.06
Outcrop-floodplain	Void filled	150	-0.4	0.4
Outcrop-floodplain	Non- Void filled	147	-0.14	0.4
Bathymetric	Void filled	678	-0.16	0.37
Bathymetric	Non-Void filled	628	-0.05	0.19

Table 4 Summary of all GPS validation statistics for River John TB-lidar DEM. SD – Standard deviation of the difference in elevation (GPS-lidar DEM).

The major reason for some higher mean and standard deviation measures for the points in dense vegetation is that the lidar could not penetrate thick grass and get the actual ground. There was a difference of about 30 cm between the Z of the GNSS check points and lidar points from all scanners. Due to larger footprint of the bathymetric scanner it was observed to penetrate thick grass better than the topographic scanner (Figure 3.6).

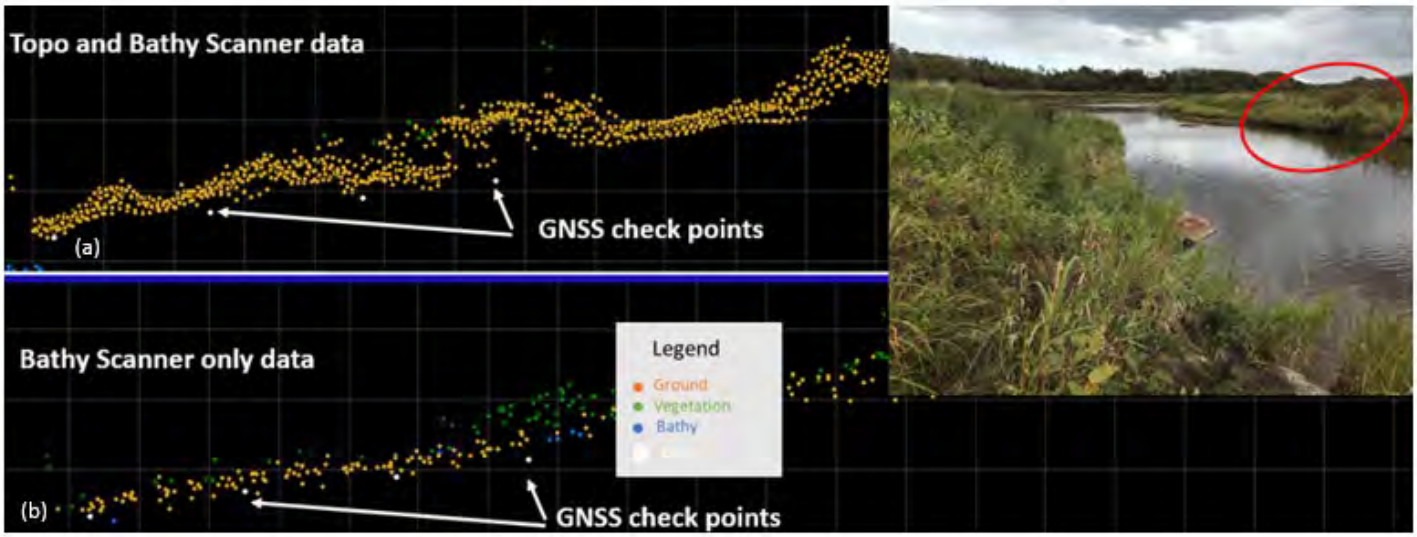

Figure 3.6 Difference in Z between GNSS check points and classified lidar point data. (a) All scanners lidar data compared to GNSS check points in outcrop as shown in the picture on the right (b) lidar data from only the bathy scanner shows it penetrates better in dense vegetation.

3.5.2 Hydrodynamic modelling validation

Results from the MIKE model were extracted at the pressure sensor locations to compare the simulated data with the observed data for the Deepwater and river model domains (Figure 3.7).

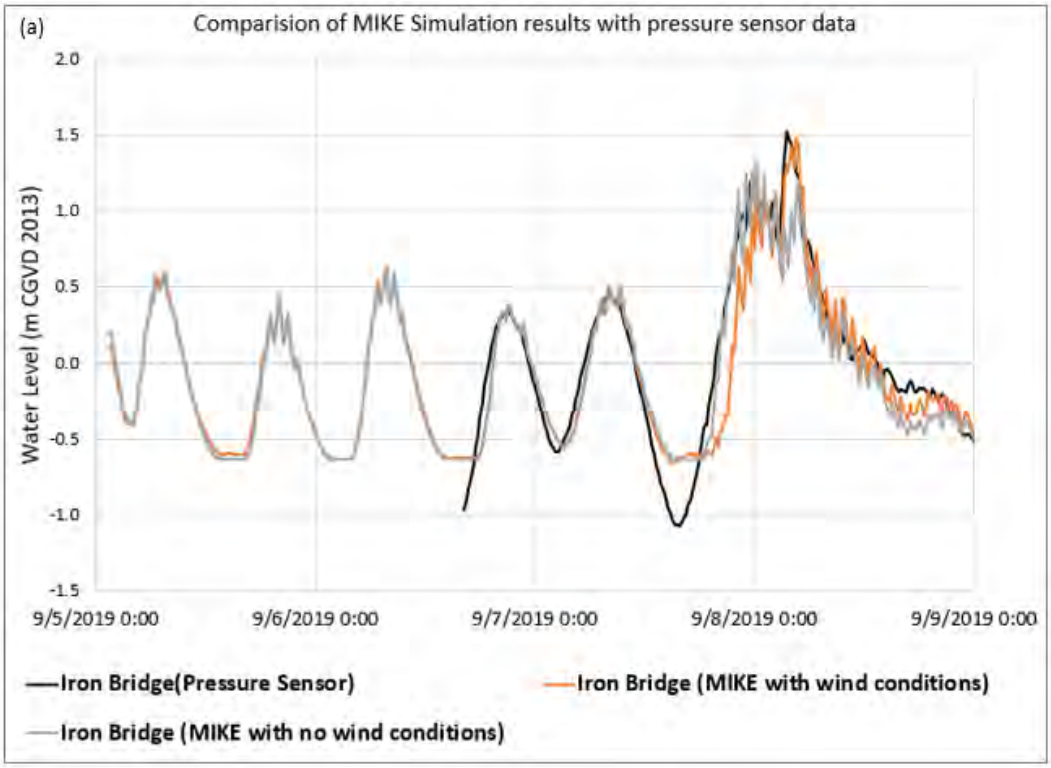
(a)
Comparision of MIKE Simulation results with pressure sensor data
Water Level (m CGVD 2013)
2.0
1.5
1.0
0.5
0.0
-0.5
-1.0
-1.5
9/5/2019 0:00
9/6/2019 0:00
9/7/2019 0:00
9/8/2019 0:00
9/9/2019 0:00
Iron Bridge(Pressure Sensor)
Iron Bridge (MIKE with wind conditions)
Iron Bridge (MIKE with no wind conditions)

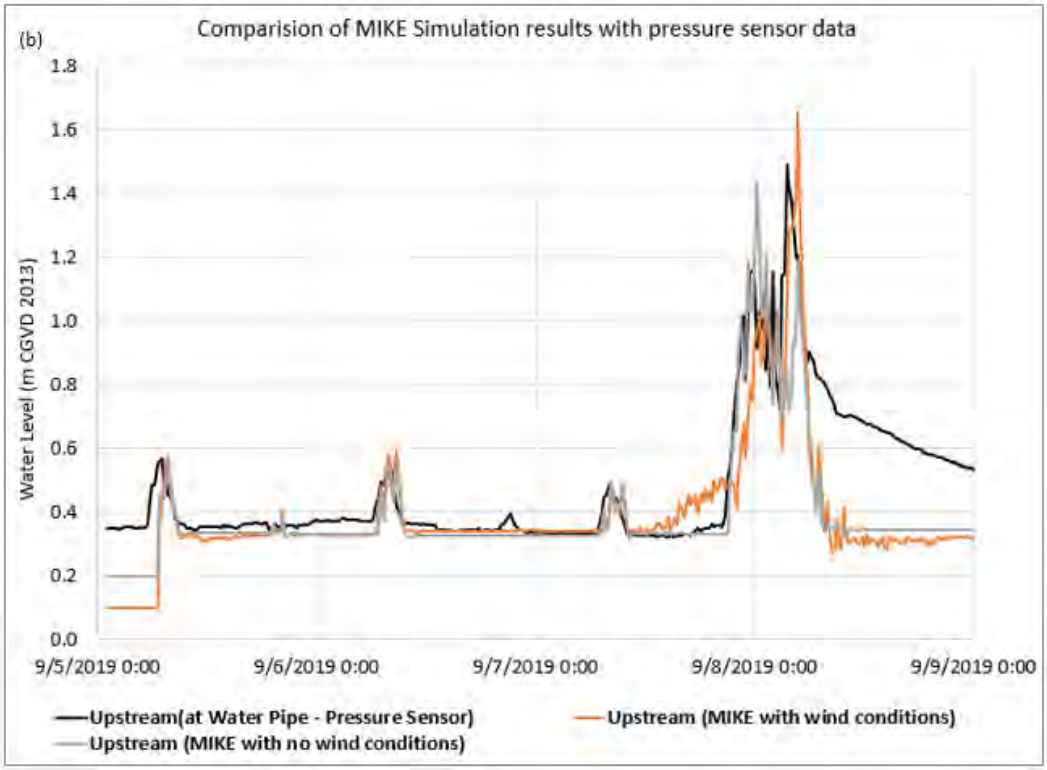
(b)
Comparision of MIKE Simulation results with pressure sensor data
Water Level (m CGVD 2013)
1.8
1.6
1.4
1.2
1.0
0.8
0.6
0.4
0.2
0.0
9/5/2019 0:00
9/6/2019 0:00
9/7/2019 0:00
9/8/2019 0:00
9/9/2019 0:00
Upstream(at Water Pipe - Pressure Sensor)
Upstream (MIKE with wind conditions)
Upstream (MIKE with no wind conditions)

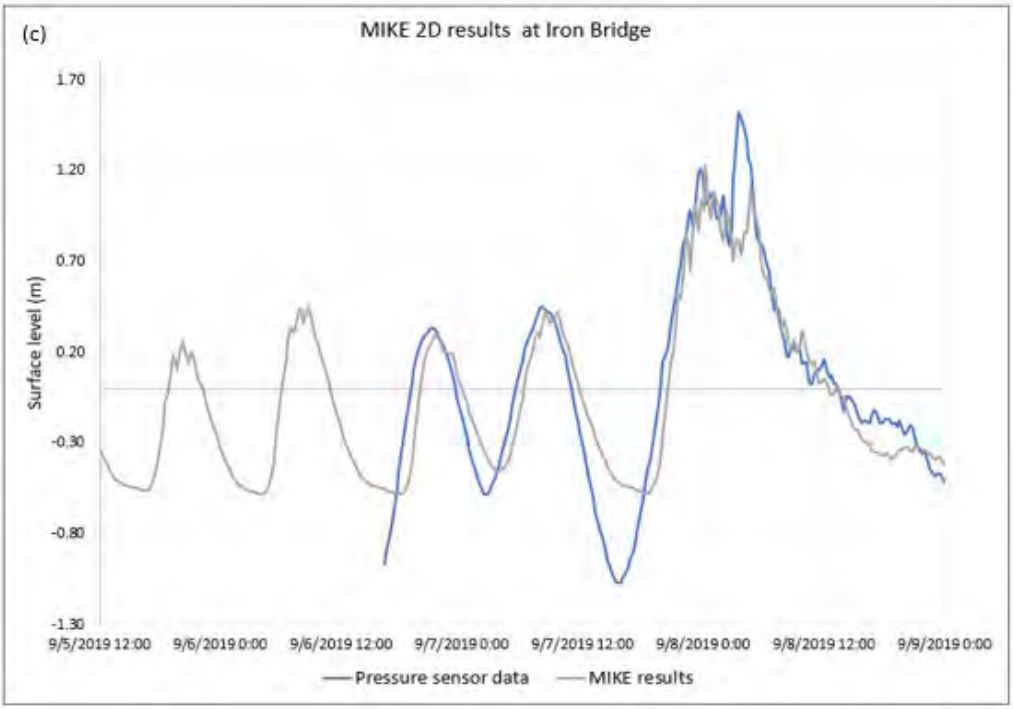

Figure 3.7 Simulation results compared with real time date from pressure sensors (a & b) results obtained from the deep water model at Iron bridge and upstream (c) results from MIKE 2D for the river model compared with pressure sensor data at Iron Bridge.

From Figure 3.7 there is a small-time lag between the simulation results and pressure sensors, the levels at low tide are about 50 cm different but the levels at high tide which are predominate for flooding match the results.

4 Discussion

We will continue to explore the enhancements that TB-lidar can provide for coastal, estuarine and river flood modelling projects. Although the TB-lidar was delayed several times as a result of aircraft delays, a successful survey was completed in late October, not during ideal conditions but sufficient to produce a high-quality seamless land-bathymetric DEM. These data have been validated and show a high level of accuracy for both exposed ground and submerged terrain. Higher levels of variance exist in the floodplain where dense vegetation obscures the ground. This is true for both topographic lidar and TB-lidar surveys, although it should be pointed out that the wider footprint of the green laser appears to penetrate the dense vegetation better than the narrower NIR laser. The water level sensors and weather station operated by AGRG-NSCC proved very useful at capturing the Hurricane Dorian event which was used to validate the modelling results. The coupled 1-D and 2-D model demonstrates the need for such an approach for estuarine environments where the freshwater run-off mixes with elevated tidal levels during such storm events when flooding typically occurs. Overall the project was very successful to demonstrating how TB-lidar can be used to enhance an inland flood

model. Future efforts will involve comparing modelling results using data from just a topographic lidar survey conducted in July 2018. In the upper reaches of the river system where the water is shallow, the topographic lidar may come close to estimating the river channel, although there is no way to identify the thalweg or other morphological features in the riverbed using these data. However, as one moves downstream and the river depth increases and the floodplain broadens, TB-lidar clearly shows the advantages for capturing the critical geometry of the riverbed and floodplain. Additional benefits to utilizing data from a TB-lidar survey include the orthophoto that is captured synchronously with the lidar during the survey and additional derived products such as submerged aquatic vegetation and bed roughness that can better parameterize flood models.

5 Conclusions

This project has successfully demonstrated how a river-estuarine TB-lidar survey can be conducted and used to support 1-D and couple 2-D flood inundation mapping. The results of a hydrodynamic model simulation consist of both water level outs and flow velocity. These two outputs can be combined to produce a flood hazard map which depicts both water depth and water speed. Most of our population and critical infrastructure are located along the coast and up estuaries. This project has demonstrated where TB-lidar can be used to supplement provincial topographic lidar coverage to better map the seamless terrain and thus populate flood models for more accurate predictions. Hurricane Dorian was captured by AGRG weather station and three water level sensors located along the open ocean coast of the Northumberland Strait, an intertidal area (Iron Bridge) and an are upstream but still influence by the higher tides (Water Pipe). Tis event was used to validate the flood model and simulate flooding conditions. Additional simulations were constructed using an estimated 100 year return period rainfall event considering climate change (RPC 8.5) in 2100 and a major flooding event where the 100 year values have been increased three times. Validation of the lidar data shows excellent agreement between the lidar and survey grade GNSS check points for open cleared areas on land and the submerged riverbed. The validation also highlights a limitation of all lidar systems that are used to capture data in the summer and fall when the ground vegetation is dense and still standing. In this case the floodplain adjacent to the river is covered by tall (~ 1 m variable) grasses and shrubs that are so dense the last lidar return, classified as ground, does not actually make it to the ground and thus the ground is positively biased in the DEM. We observed a high difference in elevation offsets and variance in in the lidar products along the floodplain as compared to the river channel and open areas. These are important considerations for users of the provincial lidar coverage when interpreting the results from flood models.

6 References

Canadian Hydrographic Services. 2019. https://www.dfo-mpo.gc.ca/science/hydrographyhydrographie/data-acquisition-eng.html

DHI Water & Environment. 2008. Mike 21 Flow Model Hints and Recommendations in Applications with Significant Flooding and Drying.

Farr, T. G., et al. 2007. The Shuttle Radar Topography Mission, Rev. Geophys., 45, RG2004, doi:10.1029/2005RG000183.

Wahba, G. 1990. Spline models for Observational data. Paper presented at CBMS-NSF Regional Conference Series in Applied Mathematics. Philadelphia: Soc. Ind. Appl. Maths.

Webster, T., Crowell, N. and Kodavati, D. 2020. Topo-bathymetric lidar for coastal and in-land flood assessment. Nova Scotia Department of Municipal Affairs. Technical report, Applied Geomatics Research Group, NSCC Middleton, NS.

Webster, T. 2017. "Advanced Coastal Mapping to Support Hydrodynamic Modelling: Final Report" Technical report, submitted to Offshore Energy Research Association and the Canadian Association of Petroleum Producers. Applied Geomatics Research Group, NSCC Middleton, NS.

Webster, T., McGuigan, K., Crowell, N., Collins, K. and MacDonald, C. 2016. Optimization of data collection and refinement of post-processing techniques for Maritime Canada's first shallow water topographic-bathymetric lidar survey. Journal of Coastal Research. Special issue on Advances in Topo-Bathymetric lidar. Vol 76: doi:10.2112/SI76-004, pp. 31-43.

WSP. 2020. Nova Scotia Municipal Flood Line Mapping: Test Case #1: Pictou, River John. Technical report submitted to NS Department of Municipal Affairs.